Hindawi Publishing Corporation
Mathematical Problems in Engineering
Volume 2012, Article ID 392197, 30 pages
doi:10.1155/2012/392197

Research Article

Modeling and Optimization of Cement Raw Materials Blending Process

Xianhong Li,[1,2] Haibin Yu,[1] and Mingzhe Yuan[1]

[1] *Department of Information Service and Intelligent Control, Shenyang Institute of Automation, Chinese Academy of Sciences, Shenyang 110016, China*
[2] *Graduate School of Chinese Academy of Sciences, University of Chinese Academy of Sciences, Beijing 100039, China*

Correspondence should be addressed to Haibin Yu, yhb@sia.cn

Received 6 May 2012; Revised 24 July 2012; Accepted 8 August 2012

Academic Editor: Hung Nguyen-Xuan

This paper focuses on modelling and solving the ingredient ratio optimization problem in cement raw material blending process. A general nonlinear time-varying (G-NLTV) model is established for cement raw material blending process via considering chemical composition, feed flow fluctuation, and various craft and production constraints. Different objective functions are presented to acquire optimal ingredient ratios under various production requirements. The ingredient ratio optimization problem is transformed into discrete-time single objective or multiple objectives rolling nonlinear constraint optimization problem. A framework of grid interior point method is presented to solve the rolling nonlinear constraint optimization problem. Based on MATLAB-GUI platform, the corresponding ingredient ratio software is devised to obtain optimal ingredient ratio. Finally, several numerical examples are presented to study and solve ingredient ratio optimization problems.

1. Introduction

Cement is a widely used construction material in the world. Cement production will experience several procedures which include raw materials blending process and burning process, cement clinker grinding process, and packaging process. Cement raw material and cement clinkers mainly contain four oxides: calcium oxide or lime (CaO), silica (SiO_2), alumina (Al_2O_3), and iron oxide (Fe_2O_3). The cement clinkers quality is evaluated by the above four oxides. Hence, ingredient ratio of cement raw material will affect the quality and property of cement clinker significantly. Optimal ingredient ratio will promote and stabilize cement quality and production craft. Therefore, cement raw materials should be reasonably mixed. Hence, it is a significant problem to obtain optimal ingredient ratio.

Many publications have studied various cement processes in cement production. In [4], under different ball charge filling ratios, ball sizes, and residence time, a continuous ball mill is studied for optimizing cement raw material grinding process. In [5], an adaptive control framework is presented for raw material blending process, and corresponding optimal control structure is discussed too. In [6, 7], control strategies are presented for cement raw material blending process by the least square methods, neural network methods, and adaptive neural-fuzzy inference methods. In [8–10], model identification and advanced control problems have been discussed, through considering chemical composition variations disturbance, and model predictive controller is used to calculate optimal raw material feed ratio. In [11], a time-varying Kalman filter is proposed to recursive estimate oxide composition of cement raw material via X-ray analysis. In [12], a T-S fuzzy controller is proposed to improve real-time performances in blending process. In [13], the feeder, ball mill, and homogenizing silo are seen as a whole system, input and output data are used to analyze blending process. In [1, 14, 15], fuzzy neural network with particle swarm optimization (FNN-PSO) methods and artificial neural network (ANN) are applied to establish and optimize cement raw material blending process. In [2, 16–24], algebraic methods, least square methods, neural network methods, linear program methods, and empirical methods are used to compute or obtain optimal ingredient ratios in cement raw material blending process. In [3, 25–28], new original raw materials and instruments are introduced in blending process. In [29–33], cement production problems are discussed.

This does not give much attention to modeling and obtaining optimal ingredient ratio in blending process. In this paper, ingredient ratio optimization problem is analyzed for cement raw material blending process under various conditions. A G-NLTV model is established for cement raw material blending process. The ingredient ratio optimization problem can be equivalently transformed into convex problems. A framework of grid interior point method is proposed to solve ingredient ratio optimization problem. A software is developed to solve the ingredient ratio optimization problem through MATLAB-GUI. This paper is arranged as follows: raw material blending process and critical cement craft parameters are introduced in Section 2; G-NLTV model of raw material blending process under various circumstances is established in Section 3; the grid interior point method framework and cement ingredient software are presented in Section 4; numerical examples in blending process are presented in Section 5; paper contents are concluded in Section 6.

2. Raw Material Blending Process and Critical Cement Craft Parameters

Cement production process could be roughly divided into three stages. The first stage is to make cement raw material, which contains raw material blending process and grinding process. The second stage and third stage are to burn the raw material and grind cement clinkers respectively. The cement raw material blending process is an important link because the blending process will affect the cement clinker quality and critical cement craft parameters, thus the blending process finally affects the cement quality. Figure 1 demonstrates cement raw material blending process and its control system. Cement original materials are usually the limestone, steel slag, shale, sandstone, clay, and correct material. The original cement materials should be blended in a reasonable proportion, and then original cement materials are transported into the ball mill which grinds original cement materials

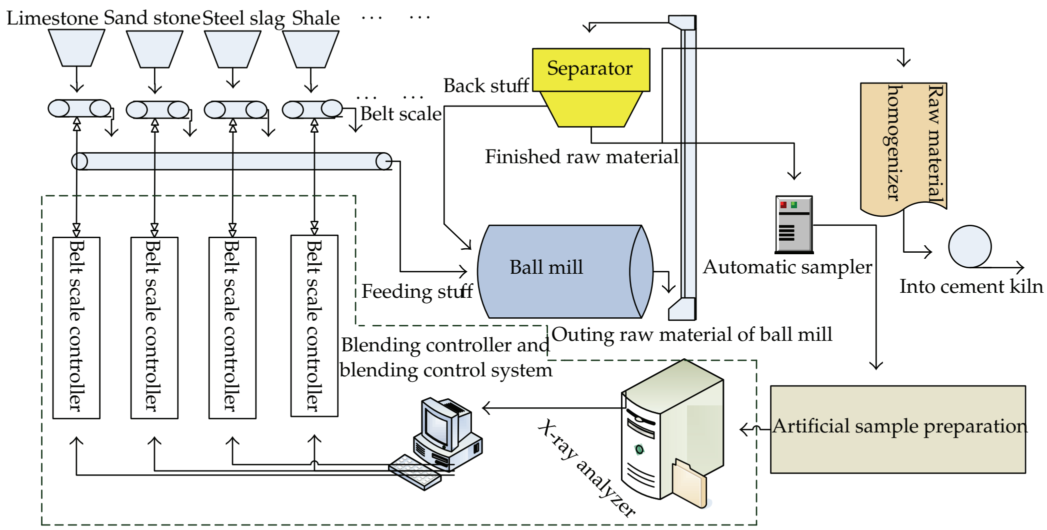

Figure 1: The cement raw material blending process and its control system.

into certain sizes. The classifier selects suitable size of original cement material which is transported to the cement kiln for burning.

The quality of cement raw material and cement clinkers are evaluated by the cement lime saturation factor (LSF), silicate ratio (SR), and aluminum-oxide ratio (AOR). LSF, SR, and AOR are directly determined by the lime, silica, alumina, and iron oxide which are contained in cement raw material. The LSF, SR, and AOR are critical cement craft parameters, thus ingredient ratio determines critical cement crafts parameters. Likewise, critical cement craft parameters are also used to assess the blending process. In cement production, the LSF, SR, and AOR must be controlled or stabilized in reasonable range. Critical cement craft parameters are not stabilized, so it cannot produce high qualified cement. The X-ray analyzer in Figure 1 is used to analyze chemical compositions of the original cement material or raw material, then X-ray analyzer can feedback LSF, SR, and AOR in fixed sample time. The LSF, SR, and AOR can be affected by many uncertain factors such as composition fluctuation, and material feeding flow. Table 1 shows the chemical composition of original cement materials. Chemical composition is the time-varying function. The symbols $\mu_j = \mu_j(t)$, $\eta_j = \eta_j(t), \ldots,$ $\omega_j = \omega_j(t)$, and $\varphi_j = \varphi_j(t)$ represent chemical composition of original cement material-j. In Table 1, R_2O represents total chemical composition of sodium oxide (Na_2O) and potassium (K_2O).

Why chemical composition is the time-varying function? Original cement materials are obtained from nature mine, thus chemical composition is time-varying function. Composition fluctuation is inevitable and it may contain randomness. With economic development, resource consumption is expanding and the resources are consuming. Therefore, original cement materials with stable chemical composition become more and more difficult to find. From the perspective of protecting environment, cement production needs to use parts of waste and sludge, therefore original cement materials composition fluctuation will be enlarged in the long run.

To some extent, modelling and optimization of the cement raw material blending process becomes more important and challenge. Because of different original cement material

Table 1: The chemical composition of cement original material.

Composition of the original cement material		SiO_2 (%)	Al_2O_3 (%)	Fe_2O_3 (%)	CaO (%)	MgO (%)	R_2O (%)	SO_3 (%)	TiO_2 (%)	Cl (%)	Impurity (%)	Loss (%)
Cement material type	Material-1	μ_1	η_1	ρ_1	γ_1	τ_1	r_1	s_1	λ_1	π_1	ω_1	φ_1
	Material-2	μ_2	η_2	ρ_2	γ_2	τ_2	r_2	s_2	λ_2	π_2	ω_2	φ_2
	$\cdots$	$\cdots$	$\cdots$	$\cdots$	$\cdots$	$\cdots$	$\cdots$	$\cdots$	$\cdots$	$\cdots$	$\cdots$	$\cdots$
	Material-i	μ_i	η_i	ρ_i	γ_i	τ_i	r_i	s_i	λ_i	π_i	ω_i	φ_i
	$\cdots$	$\cdots$	$\cdots$	$\cdots$	$\cdots$	$\cdots$	$\cdots$	$\cdots$	$\cdots$	$\cdots$	$\cdots$	$\cdots$
	Material-n	μ_n	η_n	ρ_n	γ_n	τ_n	r_n	s_n	λ_n	π_n	ω_n	φ_n
Description		Active ingredients in cement				Harmful ingredients in cement						

type, different chemical composition, and different requirements on critical cement craft parameters, ingredient ratio should be more scientific and reasonable in blending process. Therefore, ingredient ratio should adapt to the chemical composition fluctuation and guarantee critical cement craft parameters in permissible scope.

3. General Dynamic Model of Blending Process

The blending process is to produce qualified cement raw material. In cement raw material blending process, it is a key task to stabilize critical cement craft parameters LSF, SR, and AOR in permissible scope. In practice, formulas in [26, 34] are used to calculate LSF, SR, and AOR as follows:

$$\begin{gathered}
\alpha = \frac{\left(M_{\gamma} - 1.65M_{\eta} - 0.35M_{\rho}\right)}{\left(2.8M_{\mu}\right)}, \\
\text{or: } \alpha = \frac{M_{\gamma}}{\left(2.8M_{\mu} + 1.18M_{\eta} + 0.65M_{\rho}\right)}, \\
\beta = \frac{M_{\mu}}{\left(M_{\eta} + M_{\rho}\right)}, \qquad \Omega = \frac{M_{\eta}}{M_{\rho}},
\end{gathered} \tag{3.1}$$

where α is the LSF, β is the SR, and Ω is the AOR. Without losing generality, it assumes that there has n-type the original cement materials in blending process. The mass of CaO, SiO_2, Al_2O_3, and Fe_2O_3 in cement raw material can be acquired as

$$\begin{gathered}
M_{\gamma} = \gamma_1 M_1 + \cdots + \gamma_n M_n = \sum_{j=1}^{n} \gamma_j M_j, \\
M_{\mu} = \mu_1 M_1 + \cdots + \mu_n M_n = \sum_{j=1}^{n} \mu_j M_j, \\
M_{\eta} = \eta_1 M_1 + \cdots + \eta_n M_n = \sum_{j=1}^{n} \eta_j M_j, \\
M_{\rho} = \rho_1 M_1 + \cdots + \rho_n M_n = \sum_{j=1}^{n} \rho_j M_j.
\end{gathered} \tag{3.2}$$

LSF, SR, and AOR are affected by the original cement materials mass or mass percentage. Obviously, LSF, SR, and AOR are affected by composition fluctuation. Equation (3.2) is equivalently expressed as

$$\frac{M_\gamma}{M}=\frac{\left(\sum_{j=1}^{n}\gamma_j M_j\right)}{M},\qquad \frac{M_\mu}{M}=\frac{\left(\sum_{j=1}^{n}\mu_j M_j\right)}{M}$$
$$\frac{M_\eta}{M}=\frac{\left(\sum_{j=1}^{n}\eta_j M_j\right)}{M},\qquad \frac{M_\rho}{M}=\frac{\left(\sum_{j=1}^{n}\rho_j M_j\right)}{M} \tag{3.3}$$
$$M=M_1+M_2+\cdots+M_{n-1}+M_n=\sum_{j=1}^{n}M_j,$$

where M is total mass of original cement material. Variables are normalized, and (3.3) is further expressed as

$$m_\gamma=\sum_{j=1}^{n}\gamma_j x_j=\left(\gamma^T x\right),\qquad m_\mu=\sum_{j=1}^{n}\mu_j x_j=\left(\mu^T x\right),$$
$$m_\eta=\sum_{j=1}^{n}\eta_j x_j=\left(\eta^T x\right),\qquad m_\rho=\sum_{j=1}^{n}\rho_j x_j=\left(\rho^T x\right), \tag{3.4}$$
$$\sum_{j=1}^{n}x_j=1,\quad x_j=\left(\frac{M_j}{M}\right),\ x=(x_1,\ldots,x_n)^T,$$

where x_j $(j=1,\ldots,n)$ is the mass percentage of original cement material-j, $x=(x_1,\ldots,x_n)^T$ is ingredient ratio (mass percentage vector), and γ, μ, η, and ρ are mass percentage vector of CaO, SiO_2, Al_2O_3, and Fe_2O_3 for cement raw material, respectively. The ingredient ratio x is usually expressed by the percentage form, and m_γ, m_μ, m_η, $m_\rho\gamma$, μ, η, and ρ are obtained as

$$m_\gamma=\frac{M_\gamma}{M},\quad \gamma=(\gamma_1,\ldots,\gamma_n)^T,$$
$$m_\mu=\frac{M_\mu}{M},\quad \mu=(\mu_1,\ldots,\mu_n)^T,$$
$$m_\eta=\frac{M_\eta}{M},\quad \eta=(\eta_1,\ldots,\eta_n)^T, \tag{3.5}$$
$$m_\rho=\frac{M_\rho}{M},\quad \rho=(\rho_1,\ldots,\rho_n)^T.$$

In practice, each type of original cement material will possess a certain proportion, thus mass percentage x_j will yield

$$\varepsilon_j\le x_j\le 1,\quad 0\le\varepsilon_j\le 1\quad (j=1,2,\ldots,n), \tag{3.6}$$

where ε_j $(j = 1, 2, \ldots, n)$ is minimum mass percentage of original cement material-j. Minimum mass percentage ε_j is decided by cement production crafts. In cement production, the mass percentage m_γ of cement raw material should be limited in permissible scope. Otherwise, cement will lose its inherent nature property as

$$m_{\gamma-} \leq m_\gamma \leq m_{\gamma+}, \quad m_{\gamma+} = \delta_{r0} + \Delta_{r0}, \quad m_{\gamma-} = \delta_{r0} - \Delta_{r0}, \tag{3.7}$$

where $\delta_{\gamma 0}$ is the expected mass percentage of CaO, $\Delta_{\gamma 0}$ is the maximum fluctuation scope, and $m_{\gamma-}$ and $m_{\gamma+}$ are the lower bounded and upper bounded, respectively. $\delta_{\gamma 0}$ and $\Delta_{\gamma 0}$ are determined by cement production crafts. In actual cement production, critical cement craft parameters LSF, SR, and AOR should be stabilized in permissible scope as follows:

$$\alpha_{0-} \leq \alpha \leq \alpha_{0+}, \qquad \beta_{0-} \leq \beta \leq \beta_{0+}, \qquad \Omega_{0-} \leq \Omega \leq \Omega_{0+}, \tag{3.8}$$

where α_{0-}, β_{0-}, and Ω_{0-} are the minimum lower bounded of LSF, SR, and AOR respectively, and α_{0+}, β_{0+}, and Ω_{0+} are the maximum upper bounded of LSF, SR, and AOR respectively. Cement raw material is burned in the kiln, to guarantee the quality of the cement clinker, and burning loss and impurity ratio should be limited in allowable range. If raw material has too much impurity, it will affect the clinker quality. So, they can not exceed certain scope and will yield relationships as

$$\begin{gathered}
m_\varphi = \frac{M_\varphi}{M}, \quad M_\varphi = \varphi_1 M_1 + \cdots + \varphi_n M_n, \\
m_\omega = \frac{M_\omega}{M}, \quad M_\omega = \omega_1 M_1 + \cdots + \omega_n M_n, \\
m_\varphi = \varphi_1 x_1 + \cdots + \varphi_n x_n = \sum_{j=1}^{n} \varphi_j x_j = \varphi^T x \leq \delta_{\varphi 0}, \\
m_\omega = \omega_1 x_1 + \cdots + \omega_n x_n = \sum_{j=1}^{n} \omega_j x_j = \omega^T x \leq \delta_{\omega 0},
\end{gathered} \tag{3.9}$$

where $\delta_{\varphi 0}$ and $\delta_{\omega 0}$ are the maximum permission loss ratio and impurity ratio, respectively, and φ and ω are loss and impurity percentage vector, respectively. To restrict harmful ingredients and protect environment, harmful ingredients in cement raw material should be reduced as far as possible. In [29–33], it shows that too much harmful ingredients such as magnesium oxide, sodium oxide, trioxide, and potassium will affect burning process and cause cement kiln plug and crust. Harmful ingredients will affect cement clinkers quality and property. Therefore, toxic ingredients in cement raw material should be limited as follows:

$$\begin{aligned}
m_\tau &= \frac{M_\tau}{M}, \quad M_\tau = \tau_1 M_1 + \cdots + \tau_n M_n, \\
m_r &= \frac{M_r}{M}, \quad M_r = r_1 M_1 + \cdots + r_n M_n, \\
m_s &= \frac{M_s}{M}, \quad M_s = s_1 M_1 + \cdots + s_n M_n, \\
m_\lambda &= \frac{M_\lambda}{M}, \quad M_\lambda = \lambda_1 M_1 + \cdots + \lambda_n M_n, \\
m_\pi &= \frac{M_\pi}{M}, \quad M_\pi = \pi_1 M_1 + \cdots + \pi_n M_n,
\end{aligned} \tag{3.10}$$

$$\begin{aligned}
m_\tau &= \tau_1 x_1 + \cdots + \tau_n x_n = \sum_{j=1}^{n} \tau_j x_j = \tau^T x \le \delta_{\tau 0}, \\
m_r &= r_1 x_1 + \cdots + r_n x_n = \sum_{j=1}^{n} r_j x_j = r^T x \le \delta_{r0}, \\
m_s &= s_1 x_1 + \cdots + s_n x_n = \sum_{j=1}^{n} s_j x_j = s^T x \le \delta_{s0}, \\
m_\lambda &= \lambda_1 x_1 + \cdots + \lambda_n x_n = \sum_{j=1}^{n} \lambda_j x_j = \lambda^T x \le \delta_{\lambda 0}, \\
m_\pi &= \pi_1 x_1 + \cdots + \pi_n x_n = \sum_{j=1}^{n} \pi_j x_j = \pi^T x \le \delta_{\pi 0},
\end{aligned} \tag{3.11}$$

where $\delta_{\tau 0}$, δ_{r0}, δ_{s0}, $\delta_{\lambda 0}$, and $\delta_{\pi 0}$ are the permissible maximum mass percentage of MgO, R_2O, SO_3, TiO_2, and Cl in cement raw material, respectively, and τ, r, s, λ, and π are composition mass percentage vector of MgO, R_2O, SO_3, TiO_2, and Cl, respectively.

In cement production, the cement kiln can be divided into wet kiln and dry kiln. In [30–33], it shows that the cement raw material with high sulphur-alkali ratio (SAR) will cause some problems in dry kiln. Therefore, it is necessary to control the SAR for preventing cement kiln plug and crust. The cement raw material with small SAR will increase the flammability and improve the cement clinkers quality. Some formulas are presented to calculate the SAR for cement raw material. The world famous cement manufacturers such as KHD Humboldt Company, F.L.Smidth Company, and F.C.B Company in [31] propose their formulas to calculate SAR; in practice, any of the following formulas can be used to compute SAR:

$$\begin{aligned}
\text{KHD Humboldt } (\delta_{\theta 0} = 0.7\sim 1.0)\colon \theta &= \frac{M_s}{(0.85 M_{r1} + 1.29 M_{r2} - 1.119 M_\pi)} \le \delta_{\theta 0}, \\
\text{F.C.B } (\delta_{\theta 0} = 0.3\sim 1.2)\colon \theta &= \frac{M_s}{(0.85 M_{r1} + 1.29 M_{r2})} \le \delta_{\theta 0}, \\
\text{F.L.Smidth } (\delta_{\theta 0} = 0.3\%)\colon \theta &= M_s - (0.85 M_{r1} + 0.645 M_{r2}) \le \delta_{\theta 0},
\end{aligned} \tag{3.12}$$

where θ is the SAR, M_{r1} and M_{r2} are the mass or mass percentage of K_2O and Na_2O, respectively, and $\delta_{\theta 0}$ is the permissible maximum percentage. The M_{r1} and M_{r2} have the implicit relationships: $M_r = M_{r1} + M_{r2}$, $M_{r1} = \xi M_{r2}$. ξ is mass ratio between K_2O and Na_2O. The SAR is limited in permissible scope, which will reduce the environmental pollution. Strictly speaking, the blending process does not include the cement ball mill grinding process. Before cement raw materials are transported into the cement burning kiln, cement raw material blending process is considered as a whole process, thus the grinding process could be seen as part of blending process. For integrity and generality, we consider that the cement raw material blending process includes ball mill grinding process. Then, the mass balance equation of active ingredients SiO_2 in ball mill could be obtained as follows:

$$
\begin{aligned}
\frac{d(Qm_\mu)}{dt} &= F_{\text{input}} - F_{\text{output}} \Longleftrightarrow \sum_{j=1}^{n}\left(\mu_j x_j \frac{dQ}{dt} + Q\mu_j \frac{dx_j}{dt} + Qx_j \frac{d\mu_j}{dt}\right) \\
&= Q_{\text{input}} \times \sum_{j=1}^{n} \mu_j x_j - Q \times \sum_{j=1}^{n} k_{\mu,j}\mu_j x_j, \\
F_{\text{input}} &= Q_{\text{input}}\, m_\mu, \qquad F_{\text{output}} = kQm_\mu + Q \times \sum_{j=1}^{n} \nu_{\mu,j}\mu_j x_j \\
m_\mu &= \sum_{j=1}^{n} \mu_j x_j, \quad k_{\mu,j} = k + \nu_{\mu,j}, \quad (j = 1,2,\ldots,n),
\end{aligned}
\tag{3.13}
$$

where Q is original cement material output flow in ball mill, Q_{input} is original cement material feed flow, F_{input} is SiO_2 mass in feed flow, F_{output} is SiO_2 mass in output flow, and $k_{\mu,j}$ is the SiO_2 ouput mass coefficient of original cement material-j. In (3.13), it assumes that output mass is proportional to the material flow in ball mill and mass composition percentage. Likewise, the $A1_2O_3$, Fe_2O_3, and CaO mass balance equation of active ingredients in ball mill will be obtained as follows:

$$
\begin{aligned}
&\sum_{j=1}^{n}\left(\eta_j x_j \frac{dQ}{dt} + Q\eta_j \frac{dx_j}{dt} + Qx_j \frac{d\eta_j}{dt}\right) \\
&\quad = Q_{\text{input}} \times \sum_{j=1}^{n} \eta_j x_j - Q \times \sum_{j=1}^{n} k_{\eta,j}\eta_j x_j, \quad \{k_{\eta,j} = k + \nu_{\eta,j},\ (j = 1,2,\ldots,n)\}, \\
&\sum_{j=1}^{n}\left(\rho_j x_j \frac{dQ}{dt} + Q\rho_j \frac{dx_j}{dt} + Qx_j \frac{d\rho_j}{dt}\right) \\
&\quad = Q_{\text{input}} \times \sum_{j=1}^{n} \rho_j x_j - Q \times \sum_{j=1}^{n} k_{\rho,j}\rho_j x_j, \quad \{k_{\rho,j} = k + \nu_{\rho,j},\ (j = 1,2,\ldots,n)\},
\end{aligned}
$$

$$\sum_{j=1}^{n}\left(\gamma_j x_j \frac{dQ}{dt} + Q\gamma_j \frac{dx_j}{dt} + Qx_j \frac{d\gamma_j}{dt}\right)$$
$$= Q_{\text{input}} \times \sum_{j=1}^{n} \gamma_j x_j - Q \times \sum_{j=1}^{n} k_{\gamma,j}\gamma_j x_j, \quad \left\{k_{\eta,j} = k + \nu_{\gamma,j},\ (j = 1, 2, \ldots, n)\right\}. \tag{3.14}$$

Therefore, the MgO, R_2O, SO_3, TiO_2, and Cl mass balance equation of harmful ingredients in ball mill could be obtained as follows:

$$\begin{gathered}
\sum_{j=1}^{n}\left(\tau_j x_j \frac{dQ}{dt} + Q\tau_j \frac{dx_j}{dt} + Qx_j \frac{d\tau_j}{dt}\right) \\
= Q_{\text{input}} \times \sum_{j=1}^{n} \tau_j x_j - Q \times \sum_{j=1}^{n} k_{\tau,j}\tau_j x_j, \quad \left\{k_{\tau,j} = k + \nu_{\tau,j},\ (j = 1, 2, \ldots, n)\right\}, \\
\sum_{j=1}^{n}\left(r_j x_j \frac{dQ}{dt} + Qr_j \frac{dx_j}{dt} + Qx_j \frac{dr_j}{dt}\right) \\
= Q_{\text{input}} \times \sum_{j=1}^{n} r_j x_j - Q \times \sum_{j=1}^{n} k_{r,j} r_j x_j, \quad \left\{k_{r,j} = k + \nu_{r,j},\ (j = 1, 2, \ldots, n)\right\}, \\
\sum_{j=1}^{n}\left(s_j x_j \frac{dQ}{dt} + Qs_j \frac{dx_j}{dt} + Qx_j \frac{ds_j}{dt}\right) \\
= Q_{\text{input}} \times \sum_{j=1}^{n} s_j x_j - Q \times \sum_{j=1}^{n} k_{s,j} s_j x_j, \quad \left\{k_{s,j} = k + \nu_{s,j},\ (j = 1, 2, \ldots, n)\right\}, \\
\sum_{j=1}^{n}\left(\lambda_j x_j \frac{dQ}{dt} + Q\lambda_j \frac{dx_j}{dt} + Qx_j \frac{d\lambda_j}{dt}\right) \\
= Q_{\text{input}} \times \sum_{j=1}^{n} \lambda_j x_j - Q \times \sum_{j=1}^{n} k_{\lambda,j}\lambda_j x_j, \quad \left\{k_{\lambda,j} = k + \nu_{\lambda,j},\ (j = 1, 2, \ldots, n)\right\}, \\
\sum_{j=1}^{n}\left(\pi_j x_j \frac{dQ}{dt} + Q\pi_j \frac{dx_j}{dt} + Qx_j \frac{d\pi_j}{dt}\right) \\
= Q_{\text{input}} \times \sum_{j=1}^{n} \pi_j x_j - Q \times \sum_{j=1}^{n} k_{\pi,j}\pi_j x_j, \quad \left\{k_{\pi,j} = k + \nu_{\pi,j},\ (j = 1, 2, \ldots, n)\right\}.
\end{gathered} \tag{3.15}$$

The impurity and loss mass balance equation of ball mill in blending process could be also obtained as follows:

$$\sum_{j=1}^{n}\left(\omega_j x_j \frac{dQ}{dt} + Q\omega_j \frac{dx_j}{dt} + Qx_j \frac{d\omega_j}{dt}\right) = Q_{\text{input}} \times \sum_{j=1}^{n} \omega_j x_j - Q \times \sum_{j=1}^{n} k_{\omega,j}\omega_j x_j, \quad \left\{k_{\omega,j} = k + \nu_{\omega,j},\ (j = 1,2,\ldots,n)\right\}, \tag{3.16}$$

$$\sum_{j=1}^{n}\left(\varphi_j x_j \frac{dQ}{dt} + Q\varphi_j \frac{dx_j}{dt} + Qx_j \frac{d\varphi_j}{dt}\right) = Q_{\text{input}} \times \sum_{j=1}^{n} \varphi_j x_j - Q \times \sum_{j=1}^{n} k_{\varphi,j}\varphi_j x_j, \quad \left\{k_{\varphi,j} = k + \nu_{\varphi,j},\ (j = 1,2,\ldots,n)\right\}. \tag{3.17}$$

In order to obtain the general nonlinear time-varying dynamic optimization model, we needs to select suitable optimization objective function. In practice, many factors should be considered such as original cement material cost, grind ability, and the error between the actual critical craft and desired critical craft. To reduce the cement cost, an optimal ingredient ratio should be pursued to reduce the original cement material cost. Thus, original cement material cost function is acquired as

$$\min J_1 = \min\left(\sum_{j=1}^{n} x_j C_j\right) = \min\left(C^T x\right), \tag{3.18}$$

where C_j (¥/ton) is the cost of original cement material-j, and J_1 is the cost function. To improve the grind-ability, it can pursue an optimal ingredient ratio to reduce the electrical power consumption. Thus, the power consumption function is acquired as

$$\min J_2 = \min\left(\sum_{j=1}^{n} x_j P_j\right) = \min\left(P^T x\right), \tag{3.19}$$

where P_j (Kwh/ton) is bond grinding power index of original cement material-j, and J_2 is power consumption function. P_j represents the grind ability of original cement material-j and also can reflect the ball mill power consumption. To reduce critical cement craft error, it can pursue an optimal ingredient ratio to reduce LSF, SR, and AOR error. Hence, the critical cement craft error function J_3 is obtained as follows:

$$\min J_3 = \min\left\{w_1(\Delta\alpha)^2 + w_2(\Delta\beta)^2 + w_3(\Delta\Omega)^2\right\}, \quad \Delta\alpha = \alpha - \alpha_{d0}, \quad \Delta\beta = \beta - \beta_{d0}, \quad \Delta\Omega = \Omega - \Omega_{d0}, \tag{3.20}$$

where w_j $(j = 1,2,3)$ is the weight of LSF error, SR error, and AOR error, $\Delta\alpha$, $\Delta\beta$, and $\Delta\Omega$ are the error of LSF, SR, and AOR, and α_{d0}, β_{d0}, and Ω_{d0} are the expected LSF, SR, and AOR. Based

Table 2: G-NLTV dynamic optimization models of the cement raw material blending process.

Optimization models		Optimization objective functions	Constraints
Single-objective optimization	Model.1	$\min J_1 = \min(C^T x)$	(3.1)–(3.12), (3.13)–(3.17)
	Model.2	$\min J_2 = \min(P^T x)$	(3.1)–(3.12), (3.13)–(3.17)
	Model.3	$\min J_3 = \min\left\{w_1(\Delta\alpha)^2 + w_2(\Delta\beta)^2 + w_3(\Delta\Omega)^2\right\}$ (Notes: $\Delta\alpha = \alpha - \alpha_{d0}$, $\Delta\beta = \beta - \beta_{d0}$, $\Delta\Omega = \Omega - \Omega_{d0}$)	(3.1)–(3.12), (3.13)–(3.17)
Multiple-objective optimization	Model.4	$\min(J_1, J_2) = \min\{\Psi_1 J_1 + \Psi_2 J_2\}$	(3.1)–(3.12), (3.13)–(3.17)
	Model.5	$\min(J_1, J_3) = \min\{\Psi_1 J_1 + \Psi_2 J_3\}$	(3.1)–(3.12), (3.13)–(3.17)
	Model.6	$\min(J_2, J_3) = \min\{\Psi_1 J_2 + \Psi_2 J_3\}$	(3.1)–(3.12), (3.13)–(3.17)
	Model.7	$\min(J_1, J_2, J_3) = \min\{\Psi_1 J_1 + \Psi_2 J_2 + \Psi_3 J_3\}$	(3.1)–(3.12), (3.13)–(3.17)

on the cement production requirements, various objective functions are obtained. Finally, G-NLTV dynamic optimization models of cement raw material blending process are obtained as

$$\begin{gathered}
\text{Model.1: } \min J_1 = \min\left(C^T x\right) \\
\text{Model.2: } \min J_2 = \min\left(P^T x\right) \\
\text{Model.3: } \min J_3 = \min\left(w_1(\Delta\alpha)^2 + w_2(\Delta\beta)^2 + w_3(\Delta\Omega)^2\right) \\
\text{Model.4: } \min(J_1, J_2) = \min\{\Psi_1 J_1 + \Psi_2 J_2\} \\
\text{Model.5: } \min(J_1, J_3) = \min\{\Psi_1 J_1 + \Psi_2 J_3\} \\
\text{Model.6: } \min(J_2, J_3) = \min\{\Psi_1 J_2 + \Psi_2 J_3\} \\
\text{Model.7: } \min(J_1, J_2, J_3) = \min\{\Psi_1 J_1 + \Psi_2 J_2 + \Psi_3 J_3\} \\
\text{Subject to (s.t) (3.1)–(3.12), (3.13)–(3.17),}
\end{gathered} \tag{3.21}$$

where Ψ_1, Ψ_2, and Ψ_3 are the function weight. The G-NLTV dynamic optimization model includes the single objective and multiple objectives optimization model. All the optimization models contain algebraic constraints and dynamic constraints.

4. Analysis of Ingredient Ratio Optimization Problem and Grid Interior Point Framework

The object functions J_1, J_2, and J_3 in dynamic optimization models are the convex functions. The $\Psi_1 J_1 + \Psi_2 J_2, \Psi_1 J_1 + \Psi_2 J_3, \Psi_1 J_2 + \Psi_2 J_3$, and the $\Psi_1 J_1 + \Psi_2 J_2 + \Psi_3 J_3$ are also the convex functions. As known, the convex optimization problems have good convergent properties. The optimization problems are the convex optimization problem which is determined by their objective function and constraints. We need to check the constraints of optimization problems shown in Table 2. The constraints (3.1)–(3.12) are algebraic constraints and constraints (3.13)–(3.17) are dynamic constraints. The algebraic constraints and dynamic constraints construct the feasible regions of the optimization problem. The feasible region of constraint (3.12) and constraint (3.8) are obtained as

$$F_{\theta} = \left\{ x \mid \theta = \frac{M_s}{(0.85M_{r1} + 1.29M_{r2} - 1.119M_{\pi})} \le \delta_{\theta 0} \right\},$$
$$F_{\alpha,\beta,\Omega} = \left\{ x \mid \alpha_{0-} \le \alpha \le \alpha_{0+}, \beta_{0-} \le \beta \le \beta_{0+}, \Omega_{0-} \le \Omega \le \Omega_{0+} \right\}, \tag{4.1}$$

where F_{θ} and $F_{\alpha,\beta,\Omega}$ are the feasible regions constructed by constraints (3.12) and (3.8), respectively. SAR θ is equivalently expressed as

$$\theta = \frac{(M_s/M)}{((0.85M_{r1} + 1.29M_{r2} - 1.119M_{\pi})/M)}$$
$$\Longleftrightarrow \theta = \frac{m_s}{(0.85m_{r1} + 1.29m_{r2} - 1.119m_{\pi})} \tag{4.2}$$
$$\Longleftrightarrow \theta = \frac{m_s}{((0.85\xi + 1.29)m_r/(1+\xi) - 1.119m_{\pi})}.$$

Then, feasible region F_{θ} can be equivalently written as

$$F_{\theta} = \left\{ \frac{x \mid m_s}{((0.85\xi + 1.29)m_r/(1+\xi) - 1.119m_{\pi})} \le \delta_{\theta 0} \right\} \Longleftrightarrow$$
$$F_{\theta} = \{x \mid (1+\xi)m_s \le ((0.85\xi + 1.29)m_r - 1.119(1+\xi)m_{\pi})\delta_{\theta 0}\} \Longleftrightarrow \tag{4.3}$$
$$F_{\theta} = \{x \mid (1+\xi)m_s + 1.119(1+\xi)\delta_{\theta 0}m_{\pi} - (0.85\xi + 1.29)\delta_{\theta 0}m_r \le 0\}.$$

Likewise, critical cement craft parameters α, β, and Ω can be equivalently expressed as

$$\alpha = \frac{((M_{\gamma} - 1.65M_{\eta} - 0.35M_{\rho})/M)}{((2.8M_{\mu})/M)} \Longleftrightarrow$$
$$\alpha = \frac{(m_{\gamma} - 1.65m_{\eta} - 0.35m_{\rho})}{(2.8m_{\mu})}$$
$$\beta = \frac{(M_{\mu}/M)}{((M_{\eta} + M_{\rho})/M)} \Longleftrightarrow \beta = \frac{m_{\mu}}{(m_{\eta} + m_{\rho})} \tag{4.4}$$
$$\Omega = \frac{(M_{\eta}/M)}{(M_{\rho}/M)} \Longleftrightarrow \Omega = \frac{m_{\eta}}{m_{\rho}}.$$

Then, feasible region $F_{\alpha,\beta,\Omega}$ can be equivalently written as

$$\begin{aligned}
F_{\alpha,\beta,\Omega} &= \left\{ \frac{x \mid (m_\gamma - 1.65m_\eta - 0.35m_\rho)}{(2.8m_\mu)} \geq \alpha_{0-}, \frac{(m_\gamma - 1.65m_\eta - 0.35m_\rho)}{(2.8m_\mu)} \leq \alpha_{0+}, \right. \\
&\qquad \left. \frac{m_\mu}{(m_\eta + m_\rho)} \geq \beta_{0-}, \frac{m_\mu}{(m_\eta + m_\rho)} \leq \beta_{0+}, \frac{m_\eta}{m_\rho} \geq \Omega_{0-}, \frac{m_\eta}{m_\rho} \leq \Omega_{0+} \right\} \Longleftrightarrow \\
F_{\alpha,\beta,\Omega} &= \{ x \mid m_\gamma - 1.65m_\eta - 0.35m_\rho - 2.8\alpha_{0-}m_\mu \geq 0, m_\gamma - 1.65m_\eta - 0.35m_\rho - 2.8\alpha_{0+}m_\mu \leq 0, \\
&\qquad m_\mu - \beta_{0-}(m_\eta + m_\rho) \geq 0, m_\mu - \beta_{0+}(m_\eta + m_\rho) \leq 0, \\
&\qquad m_\eta - \Omega_{0-}m_\rho \geq 0, m_\eta - m_\rho\Omega_{0+} \leq 0 \} \Longleftrightarrow \\
F_{\alpha,\beta,\Omega} &= \{ x \mid m_\gamma - 1.65m_\eta - 0.35m_\rho - 2.8\alpha_{0-}m_\mu \geq 0, m_\mu - \beta_{0-}(m_\eta + m_\rho) \geq 0, m_\eta - \Omega_{0-}m_\rho \geq 0 \} \\
&\qquad \cap \{ x \mid m_\gamma - 1.65m_\eta - 0.35m_\rho - 2.8\alpha_{0+}m_\mu \leq 0, \\
&\qquad\quad m_\mu - \beta_{0+}(m_\eta + m_\rho) \leq 0, m_\eta - m_\rho\Omega_{0+} \leq 0 \}.
\end{aligned} \tag{4.5}$$

In the previous section, we know that the m_s, m_π, m_r, m_γ, m_η, m_ρ, and m_μ are the linear functions of the ingredient ratio (original cement materials mass percentage vector) $x = (x_1, x_2, \ldots, x_n)^T$. Therefore, feasible region F_θ and $F_{\alpha,\beta,\Omega}$ are the convex or semiconvex region. Constraints (3.8) and (3.12) are nonlinear algebraic constraints, but their feasible regions are also convex or semiconvex region. Hence, feasible regions constructed by constraints (3.1)–(3.12) are obtained as

$$F = \{ x \mid F_\theta \cap F_{\alpha,\beta,\Omega} \cap F_{o.e} \} \in \Pi, \tag{4.6}$$

where F is the feasible region constructed by constraints (3.1)–(3.12), $F_{o.e}$ is the feasible region constructed by constraints (3.1)–(3.10), and Π is the convex and semiconvex regions set. The constraints (3.1)–(3.10) are the linear algebraic constraints. Hence, the feasible region $F_{o.e}$ constructed by constraints (3.1)–(3.10) is the convex or semiconvex. Therefore, feasible regions constructed by constraints (3.1)–(3.12) belong to convex or semiconvex region.

The constraints (3.13)–(3.17) are the time-varying differential equation constraints in dynamic model. The constraints (3.13)–(3.17) can be equally written as the following vector form:

$$\begin{aligned}
&\frac{dQ}{dt}\mu^T x + Qx^T \frac{d\mu}{dt} + Q\mu^T \frac{dx}{dt} = Q_{\text{input}}\mu^T x - Q\mu^T \Lambda_\mu x, \quad \Lambda_\mu = \operatorname{diag}(k_{\mu,1}, \ldots, k_{\mu,n}), \\
&\frac{dQ}{dt}\eta^T x + Qx^T \frac{d\eta}{dt} + Q\eta^T \frac{dx}{dt} = Q_{\text{input}}\eta^T x - Q\eta^T \Lambda_\eta x, \quad \Lambda_\eta = \operatorname{diag}(k_{\eta,1}, \ldots, k_{\eta,n}), \\
&\frac{dQ}{dt}\rho^T x + Qx^T \frac{d\rho}{dt} + Q\rho^T \frac{dx}{dt} = Q_{\text{input}}\rho^T x - Q\rho^T \Lambda_\rho x, \quad \Lambda_\rho = \operatorname{diag}(k_{\rho,1}, \ldots, k_{\rho,n}), \\
&\frac{dQ}{dt}\gamma^T x + Qx^T \frac{d\gamma}{dt} + Q\gamma^T \frac{dx}{dt} = Q_{\text{input}}\gamma^T x - Q\gamma^T \Lambda_\gamma x, \quad \Lambda_\gamma = \operatorname{diag}(k_{\gamma,1}, \ldots, k_{\gamma,n}),
\end{aligned}$$

$$\begin{aligned}
&\frac{dQ}{dt}\tau^T x + Qx^T\frac{d\tau}{dt} + Q\tau^T\frac{dx}{dt} = Q_{\text{input}}\tau^T x - Q\tau^T\Lambda_\tau x, \quad \Lambda_\tau = \operatorname{diag}(k_{\tau,1},\ldots,k_{\tau,n}),\\
&\frac{dQ}{dt}r^T x + Qx^T\frac{dr}{dt} + Qr^T\frac{dx}{dt} = Q_{\text{input}}r^T x - Qr^T\Lambda_r x, \quad \Lambda_r = \operatorname{diag}(k_{r,1},\ldots,k_{r,n}),\\
&\frac{dQ}{dt}s^T x + Qx^T\frac{ds}{dt} + Qs^T\frac{dx}{dt} = Q_{\text{input}}s^T x - Qs^T\Lambda_s x, \quad \Lambda_s = \operatorname{diag}(k_{s,1},\ldots,k_{s,n}),\\
&\frac{dQ}{dt}\lambda^T x + Qx^T\frac{d\lambda}{dt} + Q\lambda^T\frac{dx}{dt} = Q_{\text{input}}\lambda^T x - Q\lambda^T\Lambda_\lambda x, \quad \Lambda_\lambda = \operatorname{diag}(k_{\lambda,1},\ldots,k_{\lambda,n}),\\
&\frac{dQ}{dt}\pi^T x + Qx^T\frac{d\pi}{dt} + Q\pi^T\frac{dx}{dt} = Q_{\text{input}}\pi^T x - Q\pi^T\Lambda_\pi x, \quad \Lambda_\pi = \operatorname{diag}(k_{\pi,1},\ldots,k_{\pi,n}),\\
&\frac{dQ}{dt}\omega^T x + Qx^T\frac{d\omega}{dt} + Q\omega^T\frac{dx}{dt} = Q_{\text{input}}\omega^T x - Q\omega^T\Lambda_\omega x, \quad \Lambda_\omega = \operatorname{diag}(k_{\omega,1},\ldots,k_{\omega,n}),\\
&\frac{dQ}{dt}\varphi^T x + Qx^T\frac{d\varphi}{dt} + Q\varphi^T\frac{dx}{dt} = Q_{\text{input}}\varphi^T x - Q\varphi^T\Lambda_\varphi x, \quad \Lambda_\varphi = \operatorname{diag}(k_{\varphi,1},\ldots,k_{\varphi,n}).
\end{aligned} \tag{4.7}$$

The constraints (3.13)–(3.17) in the dynamic optimization model reveal that fluctuations of the cement material flow and chemical composition will have important effects on cement raw material ingredient ratio. The derivative of ingredient ratio is affected by the chemical composition and cement material flow. In practical cement production, chemical composition is analyzed and updated by the X-ray analyzer in fixed sampling period which may be quarter hour, half hour, one hour, and even longer. Therefore, it is hard to accurately solve dynamic optimization problem (3.21) because chemical composition and cement material flow could not be continuously and accurately obtained. To simplify the dynamic model, it is assumed that the derivative of feed flow Q and ingredient ratio x are minor, and they can be ignored. Then, the constraint (4.7) can be equivalently expressed as

$$\begin{aligned}
&Qx^T\frac{d\mu}{dt} \cong Q_{\text{input}}\mu^T x - Q\mu^T\Lambda_\mu x, \qquad Qx^T\frac{d\eta}{dt} \cong Q_{\text{input}}\eta^T x - Q\eta^T\Lambda_\eta x,\\
&Qx^T\frac{d\rho}{dt} \cong Q_{\text{input}}\rho^T x - Q\rho^T\Lambda_\rho x, \qquad Qx^T\frac{d\gamma}{dt} \cong Q_{\text{input}}\gamma^T x - Q\gamma^T\Lambda_\gamma x,\\
&Qx^T\frac{d\tau}{dt} \cong Q_{\text{input}}\tau^T x - Q\tau^T\Lambda_\tau x, \qquad Qx^T\frac{dr}{dt} \cong Q_{\text{input}}r^T x - Qr^T\Lambda_r x,\\
&Qx^T\frac{ds}{dt} \cong Q_{\text{input}}s^T x - Qs^T\Lambda_s x, \qquad Qx^T\frac{d\lambda}{dt} \cong Q_{\text{input}}\lambda^T x - Q\lambda^T\Lambda_\lambda x,\\
&Qx^T\frac{d\pi}{dt} \cong Q_{\text{input}}\pi^T x - Q\pi^T\Lambda_\pi x, \qquad Qx^T\frac{d\omega}{dt} \cong Q_{\text{input}}\omega^T x - Q\omega^T\Lambda_\omega x,\\
&Qx^T\frac{d\varphi}{dt} \cong Q_{\text{input}}\varphi^T x - Q\varphi^T\Lambda_\varphi x, \quad \left(\frac{dQ}{dt}\approx 0, \frac{dx}{dt}\approx 0\right).
\end{aligned} \tag{4.8}$$

The original cement materials chemical composition will fluctuate with time. To solve the optimization problem (3.21), dynamic optimization models should be transformed into discrete form. Thus, dynamic constraint (4.8) in optimization model can be transformed into the following discrete forms:

$$\begin{gathered}\mu(k)=f_\mu(\mu(k-1),x),\qquad \eta(k)=f_\eta(\eta(k-1),x),\qquad \rho(k)=f_\rho(\rho(k-1),x),\\ \gamma(k)=f_\gamma(\gamma(k-1),x),\qquad \tau(k)=f_\tau(\tau(k-1),x),\qquad r(k)=f_r(r(k-1),x),\\ s(k)=f_s(s(k-1),x),\qquad \lambda(k)=f_\lambda(\tau(k-1),x),\qquad \pi(k)=f_\pi(\pi(k-1),x),\\ \omega(k)=f_\omega(\omega(k-1),x),\qquad \varphi(k)=f_\varphi(\varphi(k-1),x).\end{gathered}\tag{4.9}$$

It is noted $\mu(k)=\mu(kT_s),\ldots,\varphi(k)=\varphi(kT_s)$, and $x=x(k)$ in (4.9), and T_s is the sampling period. Differential equation is transformed into difference equation. Constraints (3.1)–(3.12) in dynamic optimization model are transformed into the following discrete forms:

$$\begin{gathered}h(\mu(k),\ldots,\varphi(k),x)=0\\ g(\mu(k),\ldots,\varphi(k),x)\le 0 \Longleftrightarrow\\ h(f_\mu(\mu(k-1),x),\ldots,f_\varphi(\varphi(k-1),x),x)=0\\ g(f_\mu(\mu(k-1),x),\ldots,f_\varphi(\varphi(k-1),x),x)\le 0,\end{gathered}\tag{4.10}$$

where $h(\cdot)$ and $g(\cdot)$ are the discrete equality and inequality constraint vectors, respectively. Hence, the continuous time dynamic model is transformed into the following discrete time form:

$$\begin{aligned}&\text{Model.1: } \min J_1=\min\left(C^Tx\right)\\ &\text{Model.2: } \min J_2=\min\left(P^Tx\right)\\ &\text{Model.3: } \min J_3(k,x)=\min\left(w_1(\Delta\alpha(k,x))^2+w_2(\Delta\beta(k,x))^2+w_3(\Delta\Omega(k,x))^2\right)\\ &\Delta\alpha(k,x)=\Gamma_\alpha(\gamma(k),\eta(k),\rho(k),\mu(k),x)\\ &\Delta\beta(k,x)=\Gamma_\beta(\mu(k),\eta(k),\rho(k),x)\\ &\Delta\Omega(k,x)=\Gamma_\Omega(\eta(k),\rho(k),x)\\ &\text{Model.4: } \min(J_1,J_2)=\min\{\Psi_1J_1+\Psi_2J_2\}\\ &\text{Model.5: } \min(J_1,J_3(k,x))=\min\{\Psi_1J_1+\Psi_2J_3(k,x)\}\\ &\text{Model.6: } \min(J_2,J_3(k,x))=\min\{\Psi_1J_2+\Psi_2J_3(k,x)\}\\ &\text{Model.7: } \min(J_1,J_2,J_3(k,x))=\min\{\Psi_1J_1+\Psi_2J_2+\Psi_3J_3(k,x)\}\\ &\qquad\qquad \text{s.t: (4.9)-(4.10).}\end{aligned}\tag{4.11}$$

It should be noted that (i) the continuous time dynamic optimization model is transformed into discrete time rolling optimization model; (ii) chemical composition and cement material flow cannot be obtained in a continuous and accurate way, thus it is necessary to transform the continuous model into the discrete model; (iii) it is difficult and complex to directly solve the continuous-time dynamic ingredient ratio model; (iv) the dynamic model of discrete time form is equivalent to a static optimization problem in a specific sampling time. Without losing the generality, the discrete time model can be expressed as the general form in a specific sampling period as follows:

$$\min\ f(x)\ \text{s.t:}\ h(x) = 0, \quad g(x) \le 0,\ a \le x \le b, \tag{4.12}$$

where $f(x)\colon R^n \to R$, $h(x)\colon R^n \to R^m$, and $g(x)\colon R^n \to R^q$ are the smooth and differentiable functions, x is the decision variable, and n, m, and q denote the number of the decision variables, equality constraints, and inequality constraints, respectively. The discrete model is seen as a general linear or nonlinear static optimization problem in certain sampling period. In recent years, various optimization algorithms and optimization toolboxes or softwares in [35–53] are developed to solve optimization problems. The optimization methods in [35–53] such as the Newton methods, conjugate gradient methods, steepest descent methods, interior point methods, trust region methods, quadratic programming (QP) methods, successive linear programming (SLP) methods, sequential quadratic programming (SQP) methods, genetic algorithms, and particle swarm algorithms are well established to solve constraint optimization problems. Based on interior point methods in [43–51], a framework of grid interior point method is presented for dynamic cement ingredient ratio optimization problem. The optimization problem (4.12) could be transformed into following form:

$$\begin{aligned} \min \quad & f(x) - \upsilon \sum_{i=1}^{q} \ln \delta_i \\ \text{s.t:} \quad & h(x) = 0, \quad g_\varepsilon(x) + \delta = 0 \\ & g_\varepsilon(x) = \left(g(x)^T, (a-x)^T, (x-b)^T\right)^T, \end{aligned} \tag{4.13}$$

where $\upsilon > 0$ is the barrier parameter, the slack vector $\delta = (\delta_1, \delta_2, \ldots, \delta_q)^T > 0$ is set to be positive, and $g_\varepsilon(x)$ is an expanded inequality constraint. It introduces the Lagrange multipliers y and z for barrier problem (4.13) as follows:

$$L(x, y, z, \delta) = f(x) - \upsilon \sum_{i=1}^{q} \ln \delta_i + y^T\left(g_\varepsilon(x) + \delta\right) + z^T h(x), \tag{4.14}$$

where $L(x, y, z, \delta)$ is Lagrange function, $y = (y_1, y_2, \ldots, y_q)^T$ and $z = (z_1, z_2, \ldots, z_m)^T$ are Lagrange multipliers for constraints $g_\varepsilon(x) + \delta$ and $h(x)$, respectively. Based on Karush-Kuhn-Tucker (KKT) optimality conditions [41–43], optimality conditions for optimization problem (4.13) can be expressed as

$$\begin{gathered}
\nabla_x L(x, y, z, \delta) = \nabla f(x) + \left(\nabla g_\varepsilon(x)\right)^T y + (\nabla h(x))^T z = 0, \\
\nabla_\delta L(x, y, z, \delta) = -\upsilon S_\delta^{-1} e + y = 0 \Longleftrightarrow -\upsilon e + S_\delta Y e = 0, \\
\nabla_y L(x, y, z, \delta) = g_\varepsilon(x) + \delta = 0, \\
\nabla_z L(x, y, z, \delta) = h(x) = 0,
\end{gathered} \tag{4.15}$$

where $S_\delta = \operatorname{diag}(\delta_1, \delta_2, \ldots, \delta_q)$ is the diagonal matrix and its elements are the components of the vector δ, e is a vector of all ones, $\nabla h(x)$ and $\nabla g_\varepsilon(x)$ are the Jacobian matrices of the vectors $h(x)$ and $g_\varepsilon(x)$, respectively, $\nabla f(x)$ is the grand of function $f(x)$, and $Y = \operatorname{diag}(y_1, y_2, \ldots, y_q)$ is a diagonal matrix and its elements are the components of vector y. The system (4.15) is KKT optimal condition of optimization problem (4.13). When in the search procedure, δ and y should remain positive ($\delta > 0, y > 0$). To obtain the iteration direction, we can make the point $(x + \Delta x, \delta + \Delta\delta, z + \Delta z, y + \Delta y)$ satisfy the KKT conditions (4.15), then the following system will be obtained:

$$\begin{gathered}
\nabla f(x + \Delta x) + \left(\nabla g_\varepsilon(x + \Delta x)\right)^T (y + \Delta y) + (\nabla h(x + \Delta x))^T (z + \Delta z) = 0 \\
-\upsilon e + (S_\delta + \Delta S_\delta)(Y + \Delta Y)e = 0 \\
g_\varepsilon(x + \Delta x) + (\delta + \Delta\delta) = 0, \qquad h(x + \Delta x) = 0 \Longrightarrow
\end{gathered} \tag{4.16}$$

$$\begin{gathered}
\left(\nabla^2 f(x) + \nabla^2 g_\varepsilon(x)^T y + \nabla^2 h(x)^T z\right)\Delta x + \nabla g_\varepsilon(x)^T \Delta y \\
+ \nabla h(x)^T \Delta z + \left(\nabla f(x) + \nabla g_\varepsilon(x)^T y + \nabla h(x)^T z\right) = 0, \\
-\upsilon e + S_\delta Y e + S_\delta \Delta y + Y \Delta\delta = 0, \\
g_\varepsilon(x) + \nabla g_\varepsilon(x)\Delta x + \delta + \Delta\delta = 0, \qquad \nabla h(x)\Delta x + h(x) = 0.
\end{gathered} \tag{4.17}$$

The system (4.17) is obtained by ignoring the higher order incremental system (4.16), and replacing nonlinear terms with linear approximation, system (4.17) is written in the following matrix form:

$$\begin{pmatrix} H(x, y, z) & 0 & \nabla h(x)^T & \nabla g_\varepsilon(x)^T \\ 0 & S_\delta^{-1} Y & 0 & I \\ \nabla h(x) & 0 & 0 & 0 \\ \nabla g_\varepsilon(x) & I & 0 & 0 \end{pmatrix} \begin{pmatrix} \Delta x \\ \Delta\delta \\ \Delta y \\ \Delta z \end{pmatrix} = \begin{pmatrix} -\nabla f(x) - \nabla g_\varepsilon(x)^T y - \nabla h(x)^T z \\ \upsilon S_\delta^{-1} e - y \\ -h(x) \\ -g_\varepsilon(x) - \delta \end{pmatrix} \tag{4.18}$$

$$H(x, y, z) = \nabla^2 f(x) + \nabla^2 g_\varepsilon(x)^T y + \nabla^2 h(x)^T z, \tag{4.19}$$

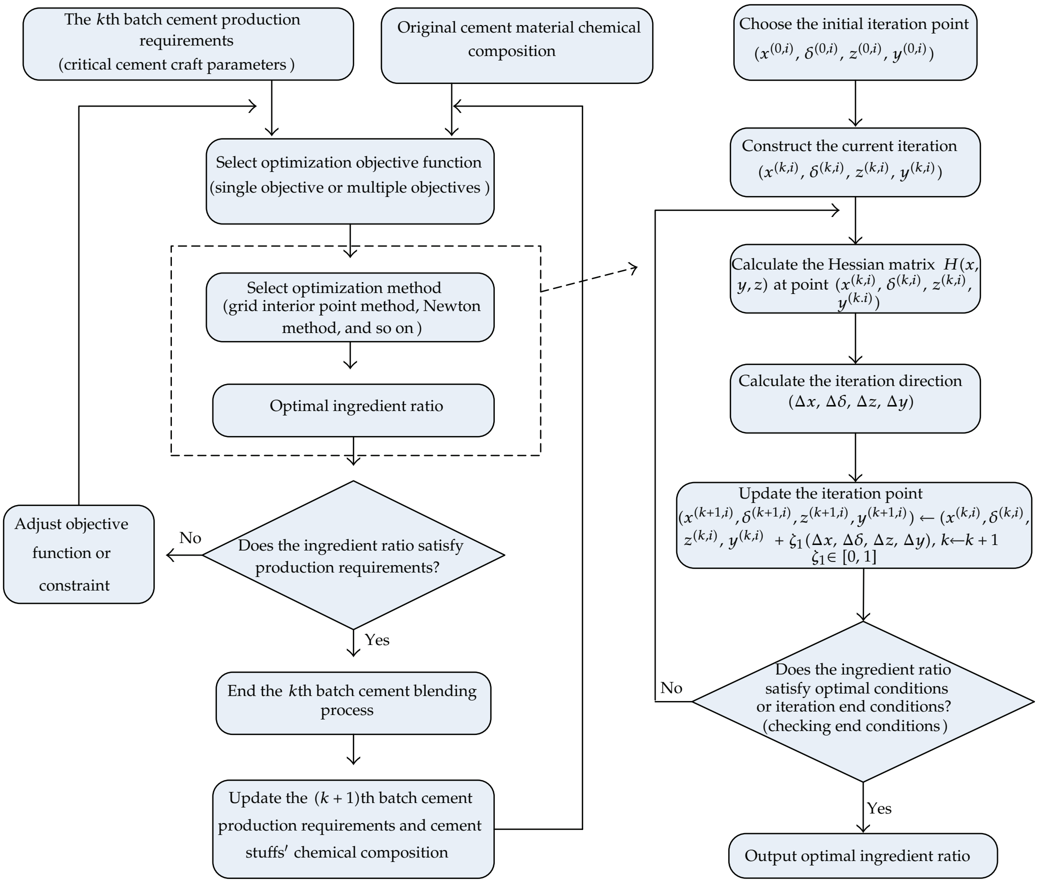

Figure 2: Optimization algorithm structure diagram of cement raw material blending process.

where $H(x, y, z)$ is the Hessian matrix in system. Finally, the new iterate direction is obtained via solving the system (4.18), which is the essential process of the interior point method. Thus, the new iteration point can be obtained in the following iteration:

$$(x, \delta, z, y) \longleftarrow (x, \delta, z, y) + \zeta_1(\Delta x, \Delta\delta, \Delta z, \Delta y), \tag{4.20}$$

where ζ_1 is the step size. Choosing the step size ζ_1 holds the $\delta, y > 0$ in search process. In this paper, a framework of grid interior point method is presented for optimization problem of ingredient ratio in raw material blending process. The grid interior point method framework is depicted as follows.

4.1. *Grid Interior Point Method Framework*

The following steps are considered.

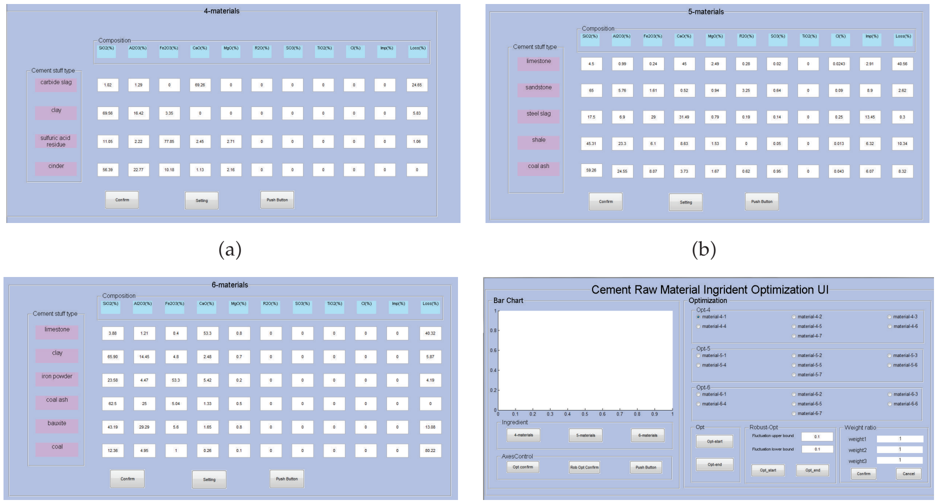

(a) (b)

(c) (d)

Figure 3: Ingredient ratio software for cement raw material blending process.

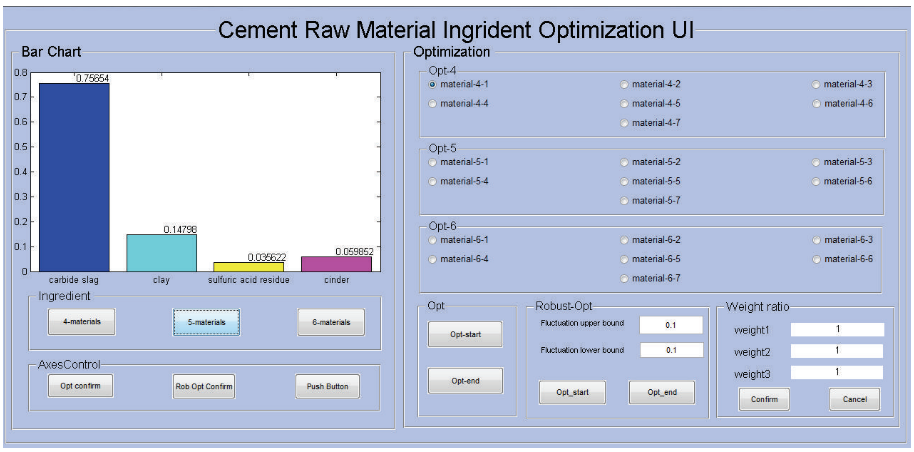

Figure 4: Optimization results of ingredient ratio software for cement raw material blending process.

Step 1. The feasible region $F = \{x \mid h(x) = 0,\ g(x) \leq 0, a \leq x \leq b\}$ is divided into N small pieces of feasible region without any intersection ($F = UF_i$), and $F_i = \{x \mid h(x) = 0,\ g(x) \leq 0,\ a + (i-1) \times \Theta \leq x \leq a + i \times \Theta\}$, and Θ is the interval length ($\Theta = (b-a)/N;\ i = 1, 2, \ldots, N$).

Step 2. For $i = 1{:}\ N$,each small feasible region will do the following steps.

Step 3. Choose an initial iteration point $(x^{(0,i)}, \delta^{(0,i)}, z^{(0,i)}, y^{(0,i)})$ in the feasible region set $F_i = \{x \mid h(x) = 0, g(x) \leq 0, a + (i-1) \times \Theta \leq x \leq a + i \times \Theta\}$, and the $\delta^{(0)} > 0,\ y^{(0)} > 0,\ k = 0$.

Step 4. Constructing current iterate, we have the current iterate value $x^{(k,i)}$, $\delta^{(k,i)}$, $z^{(k,i)}$ and $y^{(k,i)}$ of the primal variable x, the slack variable δ, and the multipliers y and z, respectively.

Table 3: Chemical compositions of cement original materials in certain sampling period [1].

Material type	SiO_2 (%)	Al_2O (%)	Fe_2O (%)	CaO (%)	Loss (%)	Impurity (%)	Power (Kwh/ton)	Cost (¥/ton)
Limestone	4.50	0.99	0.24	45.00	40.56	2.91	12.45	25.00
Sandstone	65.00	5.76	1.61	0.52	2.62	8.90	12.94	15.00
Steel slag	17.50	6.90	29.00	31.49	0.30	13.45	19.89	68.00
Shale	45.31	23.30	6.10	8.63	10.34	6.32	28.60	20.00
Coal ash	59.26	24.55	8.07	3.73	8.32	6.07	28.60	20.00

Step 5. Calculate the Hessian matrix $H(x,y,z)$ of the Lagrange system $L(x,y,z,\delta)$, and the Jacobian matrix $\nabla h(x)$ and $\nabla g(x)$ are of the vectors $h(x)$ and $g(x)$ in the current iterate $(x^{(k,i)},\delta^{(k,i)},z^{(k,i)},y^{(k,i)})$.

Step 6. Solve the linear system (4.18) and construct the iterate direction $(\Delta x,\Delta\delta,\Delta z,\Delta y)$. Solve the linear matrix equation (4.18), and then we can obtain the primal solution Δx, multipliers solution Δz, Δy, and also the slack variable solution $\Delta\delta$.

Step 7. Choosing the step size ζ_1 holds the δ, $y > 0$ in the search process, $\zeta_1 \in [0,1]$. Update the iterate values: $(x^{(k+1,i)},\delta^{(k+1,i)},z^{(k+1,i)},y^{(k+1,i)}) \leftarrow (x^{(k,i)},\delta^{(k,i)},z^{(k,i)},y^{(k,i)}) + \zeta_1(\Delta x,\Delta\delta,\Delta z,\Delta y), k \leftarrow k+1$.

Step 8. Check the ending conditions for region F_i. If it is not satisfied, go to Step 5, else the minimum $f_{\min,i}$ of feasible region F_i is obtained, $i \leftarrow i+1$, go to Step 3.

Step 9. Compare the minimum $f_{\min,i}$ of feasible region F_i, output the minimum $f_{\min} = \min\{f_{\min,i}\ (i=1,2,\ldots,N)\}$, end.

Based on the grid interior point method framework, the algorithm structure diagram of cement raw material blending process is shown in Figure 2. In this paper, we develop the ingredient ratio software for cement raw material blending process based on the MATLAB-GUI and grid interior point method. The ingredient ratio software interface is shown in Figures 3 and 4. The ingredient ratio software has strong features which include single objective optimization model, multiple objectives optimization model, and robust ingredient ratio. The software achieves ingredient ratio for four, five, and six types of original cement materials, of course the software can be further improved to achieve ingredient ratio for more types of original cement materials. In practice, it does not exceed eight types of original cement material.

5. Numerical Results for Blending Process

In production, many field operating engineers will give an ingredient ratio of original cement materials based on critical cement crafts and their experiences. In this paper, a G-NLTV model and ingredient ratio software are shown to provide optimal ingredient ratios for cement raw material blending process under different production requirements. Three numerical examples are shown to depict the proposed method. It does not consider the differential or difference equation constraint because output mass coefficient and flow of original cement materials are unknown. Tables 3–5 in the Appendix display only original cement materials

Table 4: Chemical compositions of cement original materials in certain sampling period [2].

Material type	Loss (%)	SiO_2 (%)	Al_2O_3 (%)	Fe_2O_3 (%)	CaO (%)	MgO (%)	SO_3 (%)	K_2O (%)	Na_2O (%)	Cl (%)
Limestone	40.09	8.52	1.23	1.31	46.05	2.49	0.02	0.21	0.07	0.0243
Clay	7.99	62.74	17.94	4.06	2.40	0.94	0.64	3.25	0.00	0.09
Iron	24.74	7.92	50.27	13.01	2.94	0.79	0.14	0.19	0.00	0.25
Correction	30.25	3.15	21.30	38.55	5.17	1.53	0.05	0.00	0.00	0.013
Coal ash	0.00	44.77	26.04	4.49	8.42	1.67	0.95	0.62	0.00	0.043

Assuming the cost and bond power index for the cement material in Table 4 are 24.00 ¥/ton, 25.00 ¥/ton, 50.00 ¥/ton, 30.00 ¥/ton, 28.70 ¥/ton, 12.45 Kwh/ton, 12.10 Kwh/ton, 18.98 Kwh/ton, 14.70 Kwh/ton, and 15.66 Kwh/ton, respectively.

chemical composition in a specific sampling period, wherein the chemical composition in Table 3 [1] is used to produce cement raw materials by a cement enterprise in Shan Dong province of China.

There are five types of original cement material in Table 3, and they are the limestone, sandstone, steel slag, shale, and coal ash. The steel slag is the most expensive material, the sandstone is the cheapest material, the limestone has the best grind ability, and the shale has the poorest grind ability. The optimization models (discrete time) and optimal ingredient ratios under different production requirements are presented in Table 6 and Figure 5. Model.1 has the smallest cost with the optimal ingredient ratio $x_1 = 84.003\%$, $x_2 = 7.687\%$, $x_3 = 3.203\%$, $x_4 = 0.010\%$, and $x_5 = 5.097\%$. Model.2 has the smallest power consumption with the optimal ingredient ratio $x_1 = 84.145\%$, $x_2 = 8.021\%$, $x_3 = 3.795\%$, $x_4 = 0.010\%$, and $x_5 = 4.029\%$. Model.3 has the smallest critical cement craft deviation with optimal ingredient ratio $x_1 = 84.046\%$, $x_2 = 7.335\%$, $x_3 = 3.587\%$, $x_4 = 0.010\%$, and $x_5 = 5.021\%$. Model.4, Model.5, Model.6, and Model.7 are the multiple objectives optimization model which could be equivalently transformed into single objective optimization model via introducing weight Ψ_1, Ψ_2, and Ψ_3. Model.4 makes balance between material cost and power consumption with optimal ingredient ratio $x_1 = 84.658\%$, $x_2 = 7.349\%$, $x_3 = 3.122\%$, $x_4 = 0.010\%$, and $x_5 = 4.681\%$. Model.5, Model.6, and Model.7 have the same optimal ingredient ratio with Model.1, Model.2, and Model.4, respectively because the objective function J_3 is far less than the objective function J_1 and J_2. In addition, the weight of objective function J_3 is not far larger than the weight of objective function J_1 and J_2, therefore they have the same optimal ingredient ratio.

There are five types of original cement materials in Table 4, and they are the limestone, clay, iron, correction, and coal ash. The iron is the most expensive material, the limestone is the cheapest material, the clay has the best grind ability, and the iron has the poorest grind ability. The optimization models (discrete time) and optimal ingredient ratios under different production requirements are presented in Table 7 and Figure 6. Model.1 has the smallest material cost with the optimal ingredient ratio $x_1 = 88.257\%$, $x_2 = 7.503\%$, $x_3 = 0.010\%$, $x_4 = 3.731\%$, and $x_5 = 0.499\%$. Model.2 has the smallest power consumption with the optimal ingredient ratio $x_1 = 87.565\%$, $x_2 = 8.480\%$, $x_3 = 0.040\%$, $x_4 = 3.905\%$, and $x_5 = 0.010\%$. Model.3 has the smallest critical cement craft deviation with optimal ingredient ratio $x_1 = 87.805\%$, $x_2 = 7.791\%$, $x_3 = 0.878\%$, $x_4 = 3.516\%$, and $x_5 = 0.010\%$. Model.4 makes balance between material cost and power consumption with optimal ingredient ratio $x_1 = 87.555\%$, $x_2 = 8.414\%$, $x_3 = 0.010\%$, $x_4 = 3.912\%$, and $x_5 = 0.109\%$. Model.5, Model.6, and Model.7 have the same optimal ingredient ratio with Model.1, Model.2, and Model.4, respectively.

Table 5: Chemical compositions of cement original materials in certain sampling period [3].

Material type	Loss (%)	SiO_2 (%)	Al_2O_3 (%)	Fe_2O_3 (%)	CaO (%)	MgO (%)
Carbide slag	24.65	1.02	1.29	0.00	69.26	0.00
Clay	5.83	69.56	16.42	3.35	0.00	0.00
Sulfuric acid residue	1.06	11.05	2.22	77.85	2.45	2.71
Cinder	0.00	56.39	22.77	10.18	1.13	2.16

Assuming the cost and bond power index for the cement material in Table 5 are 18.00 ¥/ton, 25.00 ¥/ton, 48.00 ¥/ton, 9.00 ¥/ton, 11.24 Kwh/ton, 12.50 Kwh/ton, 19.86 Kwh/ton, and 13.80 Kwh/ton, respectively.

Table 6: Optimization models and results for cement materials in Table 3.

	Optimization Models
	Model.1: $J_1 = 25x_1 + 15x_2 + 68x_3 + 20x_4 + 20x_5$
	Model.2: $J_2 = 12.45x_1 + 12.94x_2 + 19.89x_3 + 28.6x_4 + 28.6x_5$
	Model.3: $J_3 = w_1(1.00 - \alpha)^2 + w_2(2.70 - \beta)^2 + w_3(1.55 - \Omega)^2$
	$(w_1 = 0.5, w_2 = 0.3, w_3 = 0.2, \alpha_{d0} = 1.00, \beta_{d0} = 2.70, \Omega_{d0} = 1.55)$
	Model.4: $\min(J_1, J_2) = \min(\Psi_1 J_1 + \Psi_2 J_2)$
	Model.5: $\min(J_1, J_3) = \min(\Psi_1 J_1 + \Psi_2 J_3)$
	Model.6: $\min(J_2, J_3) = \min(\Psi_1 J_2 + \Psi_2 J_3)$
	Model.7: $\min(J_1, J_2, J_3) = \min(\Psi_1 J_1 + \Psi_2 J_2 + \Psi_3 J_3)$
	Subject to (3.1)–(3.4)
(1)	$M_\mu = 4.5x_1 + 65x_2 + 17.5x_3 + 45.31x_4 + 59.26x_5$
	$M_\eta = 0.99x_1 + 5.76x_2 + 6.9x_3 + 23.3x_4 + 24.55x_5$
	$M_\rho = 0.24x_1 + 1.61x_2 + 29.0x_3 + 6.1x_4 + 8.07x_5$
	$M_\gamma = 45.0x_1 + 0.52x_2 + 31.49x_3 + 8.63x_4 + 3.73x_5$
	$x_1 + x_2 + x_3 + x_4 + x_5 = 1.00$
	$x_1 \geq 0, x_2 \geq 0, x_3 \geq 0, x_4 \geq \varepsilon, x_5 \geq 0, (\varepsilon = 0.0001)$
(2)	$\alpha = (M_\gamma - 1.65M_\eta - 0.35M_\rho)/(2.8M_\mu)$
	$\beta = M_\mu/(M_\eta + M_\rho), \Omega = M_\eta/M_\rho$
(3)	$M_\varphi = 40.56x_1 + 2.62x_2 + 0.3x_3 + 10.34x_4 + 8.32x_5 \leq 38.00$
	$M_\omega = 2.91x_1 + 8.9x_2 + 13.45x_3 + 6.32x_4 + 6.07x_5 \leq 7.00$
(4)	$0.98 \leq \alpha \leq 1.02, 2.60 \leq \beta \leq 2.80, 1.45 \leq \Omega \leq 1.65$

Models	Optimal ingredient ratio	Notes
Model.1	$x_1^* = 84.003\%$; $x_2^* = 7.687\%$; $x_3^* = 3.203\%$; $x_4^* = 0.010\%$; $x_5^* = 5.097\%$; $J_1^* = 25.35308$;	
Model.2	$x_1^* = 84.145\%$; $x_2^* = 8.021\%$; $x_3^* = 3.795\%$; $x_4^* = 0.010\%$; $x_5^* = 4.029\%$; $J_2^* = 13.42398$;	
Model.3	$x_1^* = 84.046\%$; $x_2^* = 7.335\%$; $x_3^* = 3.587\%$; $x_4^* = 0.010\%$; $x_5^* = 5.021\%$; $J_3^* = 0.000$;	
Model.4	$x_1^* = 84.658\%$; $x_2^* = 7.349\%$; $x_3^* = 3.122\%$; $x_4^* = 0.010\%$; $x_5^* = 4.681\%$; $J_1^* + J_2^* = 38.86875$;	$\Psi_1 = \Psi_2 = 1.0$ $J_1^* = 25.36388$
Model.5	$x_1^* = 84.003\%$; $x_2^* = 7.687\%$; $x_3^* = 3.203\%$; $x_4^* = 0.010\%$; $x_5^* = 5.097\%$; $J_1^* + J_3^* = 25.35828$;	$\Psi_1 = \Psi_2 = 1.0$ $J_1^* = 25.35308$
Model.6	$x_1^* = 84.145\%$; $x_2^* = 8.021\%$; $x_3^* = 3.795\%$; $x_4^* = 0.010\%$; $x_5^* = 4.029\%$; $J_2^* + J_3^* = 13.42918$;	$\Psi_1 = \Psi_2 = 1.0$ $J_2^* = 13.42398$
Model.7	$x_1^* = 84.658\%$; $x_2^* = 7.349\%$; $x_3^* = 3.122\%$; $x_4^* = 0.010\%$; $x_5^* = 4.681\%$; $J_1^* + J_2^* + J_3^* = 38.87395$.	$\Psi_1 = \Psi_2 = \Psi_3 = 1.0$ $J_1^* = 25.36388$ $J_2^* = 13.50487$

Where x_1, x_2, x_3, x_4, and x_5 are ingredient ratio of the limestone, sandstone, steel slag, shale, and coal ash, respectively.

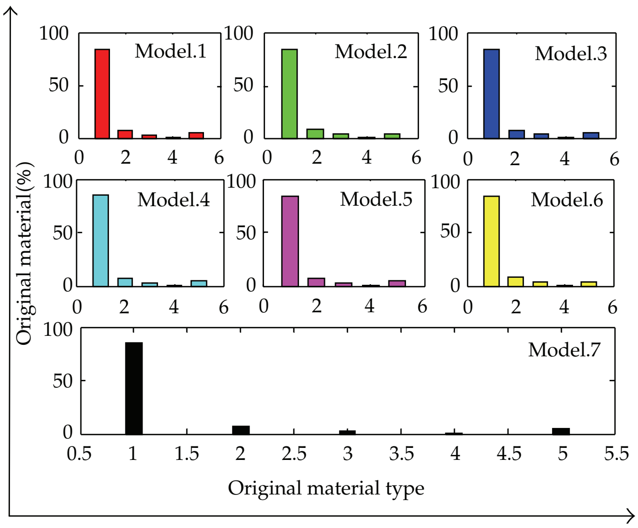

Figure 5: Optimal ingredient ratio for cement materials in Table 3.

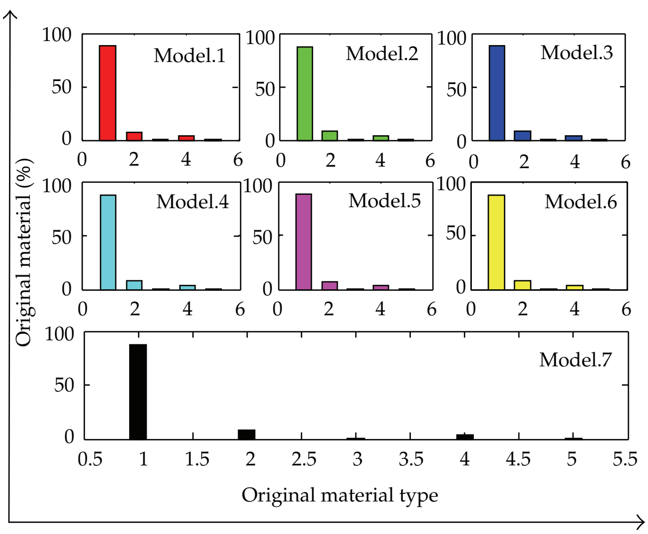

Figure 6: Optimal ingredient ratio for cement materials in Table 4.

There are four types of original cement materials in Table 5, and they are the carbide slag, clay, sulfuric acid residue, and cinder. The sulfuric acid residue is the most expensive material, the cinder is the cheapest material, the carbide slag has the best grind ability, and the sulfuric acid residue has the poorest grind ability. The optimization models (discrete time) and optimal ingredient ratios under different production requirements are presented in Table 8 and Figure 7. Model.1 has the smallest material cost with the optimal ingredient ration $x_1 = 75.007\%$, $x_2 = 14.973\%$, $x_3 = 3.620\%$, and $x_4 = 6.400\%$. Model.2 has the smallest power consumption with the optimal ingredient ratio $x_1 = 76.090\%$, $x_2 = 19.530\%$, $x_3 = 3.624\%$, and $x_4 = 0.755\%$. Model.3 has the smallest critical cement craft deviation with optimal ingredient ratio $x_1 = 75.442\%$, $x_2 = 19.623\%$, $x_3 = 4.257\%$, and $x_4 = 0.678\%$. Model.4

Table 7: Optimization models and results for cement materials in Table 4.

	Optimization Models	
	Model.1: $J_1 = 24x_1 + 25x_2 + 50x_3 + 30x_4 + 28.7x_5$	
	Model.2: $J_2 = 12.45x_1 + 12.10x_2 + 18.98x_3 + 14.70x_4 + 15.66x_5$	
	Model.3: $J_3 = w_1(0.96 - \alpha)^2 + w_2(1.90 - \beta)^2 + w_3(1.25 - \Omega)^2$	
	$(\alpha_{d0} = 0.96, \beta_{d0} = 1.90, \Omega_{d0} = 1.25, w_1 = 0.5, w_2 = 0.3, w_3 = 0.2)$	
	Model.4: $\min(J_1, J_2) = \min(\Psi_1 J_1 + \Psi_2 J_2)$	
	Model.5: $\min(J_1, J_3) = \min(\Psi_1 J_1 + \Psi_2 J_3)$	
	Model.6: $\min(J_2, J_3) = \min(\Psi_1 J_2 + \Psi_2 J_3)$	
	Model.7: $\min(J_1, J_2, J_3) = \min(\Psi_1 J_1 + \Psi_2 J_2 + \Psi_3 J_3)$	
	Subject to (3.1)–(3.5)	
(1)	$M_\mu = 8.52x_1 + 62.74x_2 + 7.92x_3 + 3.15x_4 + 44.77x_5$	
	$M_\eta = 1.23x_1 + 17.94x_2 + 50.27x_3 + 21.3x_4 + 26.04x_5$	
	$M_\rho = 1.31x_1 + 4.06x_2 + 13.01x_3 + 38.55x_4 + 4.49x_5$	
	$M_\gamma = 46.05x_1 + 2.40x_2 + 2.94x_3 + 5.17x_4 + 8.42x_5$	
	$x_1 + x_2 + x_3 + x_4 + x_5 = 1.0$, $x_1 \geq 0$, $x_2 \geq 0$, $x_3 \geq \varepsilon$, $x_4 \geq 0$, $x_5 \geq \varepsilon$, $(\varepsilon = 0.0001)$	
(2)	$\alpha = (M_\gamma - 1.65M_\eta - 0.35M_\rho)/(2.8M_\mu)$	
	$\beta = M_\mu/(M_\eta + M_\rho)$, $\Omega = M_\eta/M_\rho$	
(3)	$M_\varphi = 40.09x_1 + 7.99x_2 + 24.74x_3 + 30.25x_4 \leq 39.00$	
	$M_\tau = 2.49x_1 + 0.94x_2 + 0.79x_3 + 1.53x_4 + 1.67x_5 \leq 3.00$	
	$M_s = 0.02x_1 + 0.64x_2 + 0.14x_3 + 0.05x_4 + 0.95x_5 \leq 0.8$	
	$M_r = 0.28x_1 + 3.25x_2 + 0.19x_3 + 0.62x_5 \leq 0.9$	
	$M_{r1} = 0.21x_1 + 3.25x_2 + 0.19x_3 + 0.62x_5 \leq 0.8$, $M_{r2} = 0.07x_1 \leq 0.1$	
	$M_\pi = 0.0243x_1 + 0.09x_2 + 0.25x_3 + 0.013x_4 + 0.043x_5 \leq 0.2$	
(4)	$\theta = M_s/(0.85M_{r1} + 1.29M_{r2} - 1.119M_\pi) \leq 0.7$	
(5)	$0.94 \leq \alpha \leq 0.98; 1.80 \leq \beta \leq 2.00; 1.15 \leq \Omega \leq 1.35$	
Models	Optimal ingredient ratio	Notes
Model.1	$x_1^* = 88.257\%; x_2^* = 7.503\%; x_3^* = 0.010\%;$ $x_4^* = 3.731\%; x_5^* = 0.499\%; J_1^* = 24.32497;$	
Model.2	$x_1^* = 87.565\%; x_2^* = 8.480\%; x_3^* = 0.040\%;$ $x_4^* = 3.905\%; x_5^* = 0.010\%; J_2^* = 12.51115;$	
Model.3	$x_1^* = 87.805\%; x_2^* = 7.791\%; x_3^* = 0.878\%;$ $x_4^* = 3.516\%; x_5^* = 0.010\%; J_3^* = 0.000;$	
Model.4	$x_1^* = 87.555\%; x_2^* = 8.414\%; x_3^* = 0.010\%;$ $x_4^* = 3.912\%; x_5^* = 0.109\%; J_1^* + J_2^* = 36.83931;$	$\Psi_1 = \Psi_2 = 1$ $J_1^* = 24.32659$
Model.5	$x_1^* = 88.257\%; x_2^* = 7.503\%; x_3^* = 0.010\%;$ $x_4^* = 3.731\%; x_5^* = 0.499\%; J_1^* + J_3^* = 24.33017;$	$\Psi_1 = \Psi_2 = 1$ $J_1^* = 24.32497$
Model.6	$x_1^* = 87.565\%; x_2^* = 8.480\%; x_3^* = 0.040\%;$ $x_4^* = 3.905\%; x_5^* = 0.010\%; J_2^* + J_3^* = 12.51635;$	$\Psi_1 = \Psi_2 = 1$ $J_2^* = 12.51115$
Model.7	$x_1^* = 87.555\%; x_2^* = 8.414\%; x_3^* = 0.010\%;$ $x_4^* = 3.912\%; x_5^* = 0.109\%; J_1^* + J_2^* + J_3^* = 36.84451.$	$\Psi_1 = \Psi_2 = \Psi_3 = 1$ $J_1^* = 24.32659$ $J_2^* = 12.51273$

Where x_1, x_2, x_3, x_4, and x_5 are ingredient ratio of the limestone, clay, iron, correction materials, and coal ash, respectively.

makes balance between material cost and power consumption with optimal ingredient ratio $x_1 = 75.654\%$, $x_2 = 14.798\%$, $x_3 = 3.562\%$, and $x_4 = 5.985\%$. Model.5, Model.6, and Model.7 have the same optimal ingredient ratio with Model.1, Model.2, and Model.4, respectively.

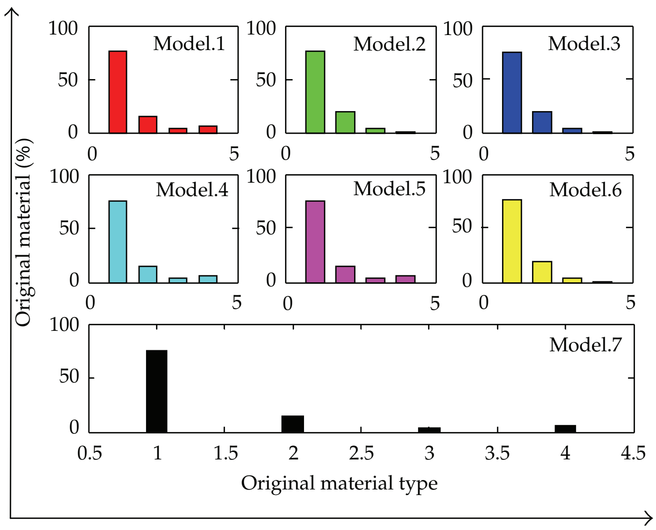

Figure 7: Optimal ingredient ratio for cement materials in Table 5.

Overall, numerical examples are presented to demonstrate various optimization problems in the blending process. The dynamic optimal ingredient ratio could be obtained in the blending process and can help to promote the cement quality if raw material chemical composition is updated with time.

6. Conclusions

This paper focuses on modelling and solving the ingredient ratio optimization problem in cement raw material blending process. A general nonlinear time-varying (G-NLTV) model of the raw material blending process is established by taking raw material chemical composition fluctuations, feed flow fluctuations, various craft constraints, and various production requirements into account. Various objective functions are presented to obtain optimal ingredient ratios under different cement production requirements. To simplify G-NLTV model and solve the optimization problem with conveniences, the optimal ingredient ratio problem is transformed into discrete time single objective rolling or multiple objectives rolling optimization problem. A framework of grid interior point method is proposed to solve the rolling optimization problem. Based on MATLAB-GUI, the corresponding ingredient ratio software is developed to achieve the optimal ingredient ratio for the cement blending process. Finally, numerical examples are shown to study and solve the ingredient ratio optimization problems in cement raw material blending process.

Appendix

See Tables 3, 4, and 5.

Table 8: Optimization models and results for cement materials in Table 5.

	Optimization Models	
	Model.1: $J_1 = 18x_1 + 25x_2 + 48x_3 + 9x_4$	
	Model.2: $J_2 = 11.24x_1 + 12.50x_2 + 19.86x_3 + 13.80x_4$	
	Model.3: $J_3 = w_1(1.02 - \alpha)^2 + w_2(1.80 - \beta)^2 + w_3(1.10 - \Omega)^2$	
	$(w_1 = 0.5, w_2 = 0.3, w_3 = 0.2, \alpha_{d0} = 1.02, \beta_{d0} = 1.80, \Omega_{d0} = 1.10)$	
	Model.4: $\min(J_1, J_2) = \min(\Psi_1 J_1 + \Psi_2 J_2)$	
	Model.5: $\min(J_1, J_3) = \min(\Psi_1 J_1 + \Psi_2 J_3)$	
	Model.6: $\min(J_2, J_3) = \min(\Psi_1 J_2 + \Psi_2 J_3)$	
	Model.7: $\min(J_1, J_2, J_3) = \min(\Psi_1 J_1 + \Psi_2 J_2 + \Psi_3 J_3)$	
	Subject to (3.1)–(3.4)	
(1)	$M_\mu = 1.02x_1 + 69.56x_2 + 11.05x_3 + 56.39x_4$	
	$M_\eta = 1.29x_1 + 16.42x_2 + 2.22x_3 + 22.77x_4$	
	$M_\rho = 3.35x_2 + 77.85x_3 + 10.18x_4$	
	$M_\gamma = 69.26x_1 + 2.45x_3 + 1.13x_4$	
	$x_1 + x_2 + x_3 + x_4 + x_5 = 1.00,\ x_1 \geq 0, x_2 \geq 0, x_3 \geq 0, x_4 \geq 0$	
(2)	$\alpha = (M_\gamma - 1.65M_\eta - 0.35M_\rho)/(2.8M_\mu)$	
	$\beta = M_\mu/(M_\eta + M_\rho),\ \Omega = M_\eta/M_\rho$	
(3)	$M_\varphi = 24.65x_1 + 5.83x_2 + 1.06x_3 \leq 30.00$	
	$M_\tau = 2.71x_3 + 2.16x_4 \leq 1.50$	
(4)	$1.00 \leq \alpha \leq 1.04, 1.70 \leq \beta \leq 1.90, 0.95 \leq \Omega \leq 1.25$	
Models	Optimal ingredient ratio	Notes
Model.1	$x_1^* = 75.007\%; x_2^* = 14.973\%; x_3^* = 3.620\%;$ $x_4^* = 6.400\%; J_1^* = 19.55801;$	
Model.2	$x_1^* = 76.090\%; x_2^* = 19.530\%; x_3^* = 3.624\%;$ $x_4^* = 0.755\%; J_2^* = 11.81783;$	
Model.3	$x_1^* = 75.442\%; x_2^* = 19.623\%; x_3^* = 4.257\%;$ $x_4^* = 0.678\%; J_3^* = 0.00000;$	
Model.4	$x_1^* = 75.654\%; x_2^* = 14.798\%; x_3^* = 3.562\%;$ $x_4^* = 5.985\%; J_1^* + J_2^* = 31.45261;$	$\Psi_1 = \Psi_2 = 1.0$ $J_1^* = 19.56587$
Model.5	$x_1^* = 75.007\%; x_2^* = 14.973\%; x_3^* = 3.620\%;$ $x_4^* = 6.400\%; J_1^* + J_3^* = 19.56571;$	$\Psi_1 = \Psi_2 = 1.0$ $J_1^* = 19.55801$
Model.6	$x_1^* = 76.090\%; x_2^* = 19.530\%; x_3^* = 3.624\%;$ $x_4^* = 0.755\%; J_2^* + J_3^* = 11.82553;$	$\Psi_1 = \Psi_2 = 1.0$ $J_2^* = 11.81783$
Model.7	$x_1^* = 75.654\%; x_2^* = 14.798\%; x_3^* = 3.562\%;$ $x_4^* = 5.985\%; J_1^* + J_2^* + J_3^* = 31.46031.$	$\Psi_1 = \Psi_2 = \Psi_3 = 1.0$ $J_1^* = 19.56587$ $J_2^* = 11.88674$

Where x_1, x_2, x_3, and x_4 are ingredient ratio of the carbide slag, clay, sulfuric acid residue, and cinder, respectively.

Nomenclature

μ_i: SiO_2 mass percentage of original cement material-*i*
η_i: Al_2O_3 mass percentage of original cement material-*i*
ρ_i: Fe_2O_3 mass percentage of original cement material-*i*
γ_i: CaO mass percentage of original cement material-*i*
τ_i: MgO mass percentage of original cement material-*i*
r_i: R_2O mass percentage of original cement material-*i*

s_i: SO_3 mass percentage of original cement material-i
λ_i: TiO_2 mass percentage of original cement material-i
π_i: Cl mass percentage of original cement material-i
ω_i: Impurity mass percentage in original cement material-i
φ_i: Mass loss percentage of original cement material-i in the cement kiln burning process
M_i: Original cement material-i mass
M_μ: SiO_2 total mass of original cement material
M_η: Al_2O_3 total mass of original cement material
M_ρ: Fe_2O_3 total mass of original cement material
M_γ: CaO total mass of original cement material
M_τ: MgO total mass of original cement material
M_r: R_2O total mass of original cement material
M_s: SO_3 total mass of original cement material
M_λ: TiO_2 total mass of original cement material
M_π: Cl total mass of original cement material
M_ω: Impurity total mass of original cement material
M_φ: Total mass loss of original cement material in cement kiln burning process
m_μ: SiO_2 total mass percentage of original cement material
m_η: Al_2O_3 total mass percentage of original cement material
m_ρ: Fe_2O_3 total mass percentage of original cement material
m_γ: CaO total mass percentage of original cement material
m_τ: MgO total mass of original cement material
m_r: R_2O total mass percentage of original cement material
m_s: SO_3 total mass percentage of original cement material
m_λ: TiO_2 total mass percentage of original cement material
m_π: Cl total mass percentage of original cement material
m_ω: Impurity total mass percentage of original cement material
m_φ: Total mass loss percentage of original cement material in cement kiln burning process.

Acknowledgments

This work is partially supported by the research project no. 2009AA04Z 155, no. KGCX2-EW-104, and no. 2010CB 334705. The authors would like to thank reviewers for their helpful suggestions.

References

[1] X. G. W, *Research and application of advanced control system in ball mill grinding process [Ph.D. thesis]*, School of Chinese Academy of Sciences, Beijing, China, 2010.
[2] H. F. Cai and Q. S. Ding, "Cement raw material ingredient based on excel calculation method," Science and Technology of Cement, No.3, 2005.
[3] L. Shi, "The ingredient plan of using carbide slag in cement production," Fujian Building Materials, No.4, 2007.
[4] R. Schnatz, "Optimization of continuous ball mills used for finish-grinding of cement by varying the L/D ratio, ball charge filling ratio, ball size and residence time," *International Journal of Mineral Processing*, vol. 74, pp. S55–S63, 2004.
[5] C. Banyasz, L. Keviczky, and I. Vajk, "A novel adaptive control system for raw material blending," *IEEE Control Systems Magazine*, vol. 23, no. 1, pp. 87–96, 2003.

[6] K. Kizilaslan, S. Ertugrul, A. Kural, and C. Ozsoy, "A comparative study on modeling of a raw material blending process in cement industry using conventional and intelligent techniques," in *Proceedings of the IEEE Conference on Control Applications*, pp. 736–741, June 2003.

[7] K. Kizilaslan, S. Ertugrul, A. Kural, and C. Ozsoy, "A comparative study on modeling of a raw material blending process in cement industry using conventional and intelligent techniques," in *Proceedings of the IEEE Conference on Control Applications*, pp. 736–741, tur, June 2003.

[8] A. Kural, *Identification and model predictive control of raw material blending process in cement industry [Ph.D. thesis]*, Institute of Science and Technology, Istanbul Technical University, Istanbul, Turkey, 2001.

[9] C. Ozsoy, A. Kural, and C. Baykar, "Modeling of the raw material mixing process in cement industry," in *Proceedings of the International Conference on Emerging Technologies and Factory Automation*, Antibes, France, October 2001.

[10] A. Kural and C. Özsoy, "Identification and control of the raw material blending process in cement industry," *International Journal of Adaptive Control and Signal Processing*, vol. 18, no. 5, pp. 427–442, 2004.

[11] M. Hubbard and T. DaSilva, "Estimation of feedstream concentrations in cement raw material blending," *Automatica*, vol. 18, no. 5, pp. 595–606, 1982.

[12] G. Bavdaz and J. Kocijan, "Fuzzy controller for cement raw material blending," *Transactions of the Institute of Measurement and Control*, vol. 29, no. 1, pp. 17–34, 2007.

[13] M. Koji, F. M. John, and U. Toshihiro, "Mixture designs and models for the simultaneous selection of ingredients and their ratios," *Chemometrics and Intelligent Laboratory Systems*, vol. 86, no. 1, pp. 17–25, 2007.

[14] X. Wu, M. Yuan, and H. Yu, "Soft-sensor modeling of cement raw material blending process based on fuzzy neural networks with particle swarm optimization," in *Proceedings of the International Conference on Computational Intelligence and Natural Computing (CINC '09)*, pp. 158–161, June 2009.

[15] Q. Pang, M. Yuan, X. Wu, and J. Wang, "Multi-objective optimization design method of control system in cement raw materials blending process based on neural network," *Dongnan Daxue Xuebao*, vol. 39, no. 1, pp. 76–81, 2009.

[16] B. Hua, K. Hua, and H. Y. Zhao, "Cement raw material ingredient based on raw material equation and excel worksheet," *Cement*, no. 3, pp. 19–22, 2002.

[17] R. P. Xing, X. H. Wang, and T. Shen, "Cement raw material ingredients algorithm based on the least-squares method?, , No," *China Cement*, no. 2, pp. 47–48, 2007.

[18] S. Y. Yang, W. W. Gao, and P. G. Jiang, "Application of neural network in cement raw materials blending system," Industry and Mine Automation, No.5, 2004.

[19] S. J. Leng, "Linear programming method application in the computational program of the cement raw material ingredient," *Cement Technology*, no. 5, pp. 33–37, 1989.

[20] Z. Q. Qiu, Q. R. Xiang, and M. Qiu, "Algebraic algorithm and its computer program of the cement raw material ingredient," *Sichuan Cement*, no. 2, pp. 8–9, 1995.

[21] C. X. Cai, "New method of simplifying the calculation of the cement raw material ingredient- raw material chemical composition ratio method," *Cement*, no. 4, pp. 20–22, 2000.

[22] Y. D. Wu, "Simple and convenient method of calculating cement raw material ingredient," *Cement Technology*, no. 4, pp. 36–40, 2001.

[23] Z. G. Zhang, X. F. Lin, and Z. Y. Wang, "The optimized control system in cement raw materials matching process," *Computing Technology and Automation*, vol. 26, no. 1, pp. 30–32, 2007.

[24] S. Chen, "Discuss optimization of the cement raw material blending process," Cement, No.6, 1995.

[25] K. J. Fan and X. M. Jin, "An overview of the raw material blending process control in cement industry," *Chinese Ceramic Society*, vol. 27, no. 4, 2008.

[26] B. Liu, X. C. Hao, and H. B. Li, "Research on the control system of the cement raw material proportioning," *Cement Technology*, no. 3, pp. 95–97, 2005.

[27] L. Li, Y. D. Wu, and C. F. Wang, "New view on the cement raw material ingredient and its control," *Liaoning Building Materials*, no. 4, pp. 20–24, 1998.

[28] R. G. Wang, "Application Analysis of the CBX analyzer in the cement raw material ingredient," *Cement*, no. 7, pp. 62–64, 2009.

[29] Q. D. Chen, *Principle and Application of the New Dry-Process Cement Technology*, China Building Industry Press, Beijing, China, 2004.

[30] H. T. Hu, "Several issues related to raw materials in new dry-process cement production," *Cement Technology*, no. 3, pp. 2–5, 1991.

[31] D. G. Su, Y. Y. Wu, S. C. Pan, H. Mai, and S. N. Pan, “Some questions of using the high sulfur-alkali materials in new dry-process cement production,” *Cement Technology*, no. 4, pp. 50–56, 1996.

[32] D. G. Su, J. Ran, B. Z. Du, H. Liu, and L. Q. Zheng, “Technical proportion for use of high sulphur-slkali ratio raw meal on dry-process cement kiln,” *Building Material of New Technology*, no. 1, pp. 5–10, 1996.

[33] D. G. Su, “Study on technical formula of high sulfur-alkali ratio materials by pass free process,” *Journal of South China University of Technology*, vol. 25, no. 7, pp. 88–92, 1997.

[34] http://www.cement.com.pk/cement-plant/raw-material-preparation.html .

[35] T. F. Coleman and Y. Li, “On the convergence of interior-reflective Newton methods for nonlinear minimization subject to bounds,” *Mathematical Programming A*, vol. 67, no. 2, pp. 189–224, 1994.

[36] D. F. Shanno, “Conditioning of quasi-Newton methods for function minimization,” *Mathematics of Computation*, vol. 24, pp. 647–656, 1970.

[37] W. W. Hager and H. Zhang, “A new conjugate gradient method with guaranteed descent and an efficient line search,” *SIAM Journal on Optimization*, vol. 16, no. 1, pp. 170–192, 2005.

[38] J. E. Dennis, Jr, M. El-Alem, and K. Williamson, “A trust-region approach to nonlinear systems of equalities and inequalities,” *SIAM Journal on Optimization*, vol. 9, no. 2, pp. 291–315, 1999.

[39] W. W. Hager and D. T. Phan, “An ellipsoidal branch and bound algorithm for global optimization,” *SIAM Journal on Optimization*, vol. 20, no. 2, pp. 740–758, 2009.

[40] N. I. M. Gould, “The generalized steepest-edge for linear programming,” Combinatorics and Optimization 83-2, University of Waterloo, Ontario, Canada, 1983.

[41] R. M. Freund, *MIT Open Courseware: Systems Optimization Models and Computation, Lecture on the “Introduction to Convex Constrained Optimization” and “Issues in Non-Convex Optimization”*, Massachusetts Institute of Technology, 2004.

[42] Y. Zhang, “Solving large-scale linear programs by interior-point methods under the MATLAB environment,” Tech. Rep. TR96-01, Department of Mathematics and Statistics, University of Maryland, Baltimore, Md, USA, 1995.

[43] R. J. Vanderbei and D. F. Shanno, “An interior-point algorithm for nonconvex nonlinear programming,” *Computational Optimization and Applications*, vol. 13, no. 1-3, pp. 231–252, 1999.

[44] H. Y. Benson and D. F. Shanno, “Interior-point methods for nonconvex nonlinear programming: regularization and warmstarts,” *Computational Optimization and Applications*, vol. 40, no. 2, pp. 143–189, 2008.

[45] R. J. Vanderbei, “LOQO: an interior point code for quadratic programming,” Tech. Rep. SOR 94-15, Princeton University, Princeton, NJ, USA, 1994.

[46] M. Gertz, J. Nocedal, and A. Sartenaer, “A starting point strategy for nonlinear interior methods,” *Applied Mathematics Letters*, vol. 17, no. 8, pp. 945–952, 2004.

[47] R. H. Byrd, J. C. Gilbert, and J. Nocedal, “A trust region method based on interior point techniques for nonlinear programming,” *Mathematical Programming*, vol. 89, no. 1, pp. 149–185, 2000.

[48] R. A. Waltz, J. L. Morales, J. Nocedal, and D. Orban, “An interior algorithm for nonlinear optimization that combines line search and trust region steps,” *Mathematical Programming A*, vol. 107, no. 3, pp. 391–408, 2006.

[49] R. H. Byrd, M. E. Hribar, and J. Nocedal, “An interior point algorithm for large-scale nonlinear programming,” *SIAM Journal on Optimization*, vol. 9, no. 4, pp. 877–900, 1999.

[50] A. Forsgren, P. E. Gill, and M. H. Wright, “Interior methods for nonlinear optimization,” *SIAM Review*, vol. 44, no. 4, pp. 525–597, 2002.

[51] A. Wachter, *An interior point algorithm for large-scale nonlinear optimization with applications in process engineering, Dissertation in Chemical Engineering [Ph.D. thesis]*, Carnegie Mellon University, Pittsburgh, Penn, USA, 2002.

[52] D. E. Goldberg, *Genetic Algorithms in Search, Optimization and Machine Learning*, Addison-Wesley, Reading, Mass, USA, 1989.

[53] H. H. Holger and T. Stutzle, *Stochastic Local Search: Foundations and Applications*, Morgan Kaufmann, San Francisco, Calif, USA, 2004.